

# Finite-difference approach to pricing barrier options under stochastic skew model

Andrey Itkin

Amaranth Group

Amaranth LLC, One American Lane, Greenwich, CT 06831, [aitkin@amaranthllc.com](mailto:aitkin@amaranthllc.com)

Peter Carr

Bloomberg L.P.

499 Park Avenue, New York, NY 10022, [PCarr4@bloomberg.com](mailto:PCarr4@bloomberg.com)

- There is a huge market for foreign exchange (FX), much larger than the equity market ... As a result, an understanding of FX dynamics is economically important.

- There is a huge market for foreign exchange (FX), much larger than the equity market ... As a result, an understanding of FX dynamics is economically important.
- Using currency option quotes, Carr and Wu (2004) found that under a risk-neutral measure, currency returns display not only stochastic volatility, but also stochastic skew.

- There is a huge market for foreign exchange (FX), much larger than the equity market ... As a result, an understanding of FX dynamics is economically important.
- Using currency option quotes, Carr and Wu (2004) found that under a risk-neutral measure, currency returns display not only stochastic volatility, but also stochastic skew.
- Using the general framework of time-changed Levy processes, they proposed a class of models (SSM) that captures both stochastic volatility and skewness.

- There is a huge market for foreign exchange (FX), much larger than the equity market ... As a result, an understanding of FX dynamics is economically important.
- Using currency option quotes, Carr and Wu (2004) found that under a risk-neutral measure, currency returns display not only stochastic volatility, but also stochastic skew.
- Using the general framework of time-changed Levy processes, they proposed a class of models (SSM) that captures both stochastic volatility and skewness.
- The models they proposed are also highly tractable for pricing and estimation. The pricing speed for European vanilla options is comparable to the speed of the Bates (1996) model.

- There is a huge market for foreign exchange (FX), much larger than the equity market ... As a result, an understanding of FX dynamics is economically important.
- Using currency option quotes, Carr and Wu (2004) found that under a risk-neutral measure, currency returns display not only stochastic volatility, but also stochastic skew.
- Using the general framework of time-changed Levy processes, they proposed a class of models (SSM) that captures both stochastic volatility and skewness.
- The models they proposed are also highly tractable for pricing and estimation. The pricing speed for European vanilla options is comparable to the speed of the Bates (1996) model.
- However, almost nothing has been done so far for exotics.

# Brief overview of the Stochastic Skew Model

- Proposed by Carr and Wu (2004) to study the variation of FX option prices in the cross section and over calendar time.



- Proposed by Carr and Wu (2004) to study the variation of FX option prices in the cross section and over calendar time.
- Like equity options, FX option implied volatilities vary stochastically over calendar time, and there is a smile in FX option implieds i.e. the convexity measure is always positive.

- Proposed by Carr and Wu (2004) to study the variation of FX option prices in the cross section and over calendar time.
- Like equity options, FX option implied volatilities vary stochastically over calendar time, and there is a smile in FX option implieds i.e. the convexity measure is always positive.
- This suggests that stochastic volatility is needed to explain risk-neutral currency dynamics, as shown for example by Bates (1996).

- Proposed by Carr and Wu (2004) to study the variation of FX option prices in the cross section and over calendar time.
- Like equity options, FX option implied volatilities vary stochastically over calendar time, and there is a smile in FX option implieds i.e. the convexity measure is always positive.
- This suggests that stochastic volatility is needed to explain risk-neutral currency dynamics, as shown for example by Bates (1996).
- However, unlike equity options, there is a substantial variation in the skewness measure as well. For both currency pairs, the skewness measure switches signs several times over our 8 year history.

- Proposed by Carr and Wu (2004) to study the variation of FX option prices in the cross section and over calendar time.
- Like equity options, FX option implied volatilities vary stochastically over calendar time, and there is a smile in FX option implieds i.e. the convexity measure is always positive.
- This suggests that stochastic volatility is needed to explain risk-neutral currency dynamics, as shown for example by Bates (1996).
- However, unlike equity options, there is a substantial variation in the skewness measure as well. For both currency pairs, the skewness measure switches signs several times over our 8 year history.
- This suggests that stochastic skewness is also needed to explain risk-neutral currency dynamics.

# SSM model (continue)

We assume frictionless markets and no arbitrage. Carr and Wu (2004) further assume that under an EMM  $\mathbb{Q}$ , the dynamics of the spot exchange rate and the two activity rates are given by the following system of SDE:

$$\begin{aligned} dS_t &= (r_d - r_f)S_{t-}dt \\ &+ \sigma\sqrt{V_t^R}S_{t-}dW_t^R + \int_0^\infty S_{t-}(e^x - 1) \left[ \mu^R(dx, dt) - \lambda \frac{e^{-|x|/\nu_j}}{|x|^{1+\alpha}} \sqrt{V_t^R} dx dt \right] \\ &+ \sigma\sqrt{V_t^L}S_{t-}dW_t^L + \int_{-\infty}^0 S_{t-}(e^x - 1) \left[ \mu^L(dx, dt) - \lambda \frac{e^{-|x|/\nu_j}}{|x|^{1+\alpha}} \sqrt{V_t^L} dx dt \right] \end{aligned}$$

$$dV_t^R = \kappa(1 - V_t^R)dt + \sigma_V \sqrt{V_t^R} dZ_t^R$$

$$dV_t^L = \kappa(1 - V_t^L)dt + \sigma_V \sqrt{V_t^L} dZ_t^L \quad (1)$$

$$dW_t^R dW_t^L = 0, \quad dZ_t^R dZ_t^L = 0, \quad dW_t^R dZ_t^L = 0, \quad dW_t^L dZ_t^R = 0$$

$$dW_t^R dZ_t^R = \rho^R dt, \quad dW_t^L dZ_t^L = \rho^L dt,$$

# SSM model - Assumptions

- Here  $t \in [0, \Upsilon]$ ,  $r_d, r_f, \sigma, \lambda, \sigma_V, \kappa$  are nonnegative constants,  $S_0, V_0^R, V_0^L, \nu_j$  are positive constants,  $\alpha < 2$  is constant,  $\rho^R, \rho^L \in [-1, 1]$  are constant,  $\Upsilon$  is some arbitrarily distant horizon.

# SSM model - Assumptions

- Here  $t \in [0, \Upsilon]$ ,  $r_d, r_f, \sigma, \lambda, \sigma_V, \kappa$  are nonnegative constants,  $S_0, V_0^R, V_0^L, \nu_j$  are positive constants,  $\alpha < 2$  is constant,  $\rho^R, \rho^L \in [-1, 1]$  are constant,  $\Upsilon$  is some arbitrarily distant horizon.
- Since the spot exchange rate can jump,  $S_{t-}$  denotes the spot price just prior to any jump at  $t$ .

# SSM model - Assumptions

- Here  $t \in [0, \Upsilon]$ ,  $r_d, r_f, \sigma, \lambda, \sigma_V, \kappa$  are nonnegative constants,  $S_0, V_0^R, V_0^L, \nu_j$  are positive constants,  $\alpha < 2$  is constant,  $\rho^R, \rho^L \in [-1, 1]$  are constant,  $\Upsilon$  is some arbitrarily distant horizon.
- Since the spot exchange rate can jump,  $S_{t-}$  denotes the spot price just prior to any jump at  $t$ .
- The processes  $W^R, W^L, Z^L, Z^R$  are all  $\mathbb{Q}$  standard Brownian motions. The random measures  $\mu^R(dx, dt)$  and  $\mu^L(dx, dt)$  are used to count the number of up jumps and down jumps of size  $x$  in the log spot FX rate at time  $t$ .



# SSM model - Assumptions

- Here  $t \in [0, \Upsilon]$ ,  $r_d, r_f, \sigma, \lambda, \sigma_V, \kappa$  are nonnegative constants,  $S_0, V_0^R, V_0^L, \nu_j$  are positive constants,  $\alpha < 2$  is constant,  $\rho^R, \rho^L \in [-1, 1]$  are constant,  $\Upsilon$  is some arbitrarily distant horizon.
- Since the spot exchange rate can jump,  $S_{t-}$  denotes the spot price just prior to any jump at  $t$ .
- The processes  $W^R, W^L, Z^L, Z^R$  are all  $\mathbb{Q}$  standard Brownian motions. The random measures  $\mu^R(dx, dt)$  and  $\mu^L(dx, dt)$  are used to count the number of up jumps and down jumps of size  $x$  in the log spot FX rate at time  $t$ .
- When calibrating, we assume that  $S_0, r_d$ , and  $r_f$  are directly observable. The parameter  $\alpha < 2$  is pre-specified. This leaves the two state variables  $V_t^R, V_t^L$  and the 7 free parameters  $\sigma, \lambda, \sigma_V, \kappa, \nu_j, \rho^R, \rho^L$  to be identified from the time series of option prices across multiple maturities and moneyness levels.

The vector process  $[S_t, V_t^R, V_t^L, t]$  is Markovian in itself on the state space  $S > 0, V_R > 0, V_L > 0, t \in [0, T)$ . Let:

$$C(S, V_R, V_L, t) \equiv e^{-r(T-t)} E^{\mathbb{Q}} \left\{ (S_T - K)^+ \middle| [S_t, V_t^R, V_t^L, t] = [S, V_R, V_L, t] \right\} \quad (2)$$

This function is governed by the following PIDE:

$$\begin{aligned} r_d C &= \frac{\partial}{\partial t} C + (r_d - r_f) S \frac{\partial}{\partial S} C + \kappa(1 - V_R) \frac{\partial}{\partial V_R} C + \kappa(1 - V_L) \frac{\partial}{\partial V_L} C \\ &+ \frac{\sigma^2 S^2 (V_R + V_L)}{2} \frac{\partial^2}{\partial S^2} C + \sigma \rho^R \sigma_V S V_R \frac{\partial^2}{\partial S \partial V_R} C + \sigma \rho^L \sigma_V S V_L \frac{\partial^2}{\partial S \partial V_L} C \\ &+ \frac{\sigma_V^2 V_R}{2} \frac{\partial^2}{\partial V_R^2} C + \sqrt{V_R} \int_0^\infty \left[ C(S e^x) - C - S(e^x - 1) \frac{\partial}{\partial S} C \right] \lambda \frac{e^{-|x|/\nu_j}}{|x|^{1+\alpha}} dx \\ &+ \frac{\sigma_V^2 V_L}{2} \frac{\partial^2}{\partial V_L^2} C + \sqrt{V_L} \int_{-\infty}^0 \left[ C(S e^x) - C - S(e^x - 1) \frac{\partial}{\partial S} C \right] \lambda \frac{e^{-|x|/\nu_j}}{|x|^{1+\alpha}} dx, \\ C &= C(S, V_R, V_L, t) \end{aligned} \quad (3)$$

# Barrier options - Boundary Conditions

- The terminal condition for the European call value is:

$$C(S, V_R, V_L, T) = (S - K)^+, \quad S \in \mathbb{R}, V_R > 0, V_L > 0$$

# Barrier options - Boundary Conditions

- The terminal condition for the European call value is:

$$C(S, V_R, V_L, T) = (S - K)^+, \quad S \in \mathbb{R}, V_R > 0, V_L > 0$$

- **Boundary conditions on  $S$**

- The terminal condition for the European call value is:

$$C(S, V_R, V_L, T) = (S - K)^+, \quad S \in \mathbb{R}, V_R > 0, V_L > 0$$

- **Boundary conditions on  $S$**

**Down and Out Calls.** On the domain  $S < L, V_R > 0, V_L > 0$  and  $t \in [0, T], C(S, V_R, V_L, t) = 0$ . We impose a zero gamma boundary condition at extremely high return levels:

$$\lim_{S \uparrow \infty} \frac{\partial^2}{\partial S^2} C(S, V_R, V_L, t) = 0, \quad V_R > 0, V_L > 0, t \in [0, T].$$

- The terminal condition for the European call value is:

$$C(S, V_R, V_L, T) = (S - K)^+, \quad S \in \mathbb{R}, V_R > 0, V_L > 0$$

- **Boundary conditions on  $S$**

**Down and Out Calls.** On the domain  $S < L, V_R > 0, V_L > 0$  and  $t \in [0, T], C(S, V_R, V_L, t) = 0$ . We impose a zero gamma boundary condition at extremely high return levels:

$$\lim_{S \uparrow \infty} \frac{\partial^2}{\partial S^2} C(S, V_R, V_L, t) = 0, \quad V_R > 0, V_L > 0, t \in [0, T].$$

**Up and Out Calls.** On the domain  $H < S, V_R > 0, V_L > 0$  and  $t \in [0, T], C(S, V_R, V_L, t) = 0$ . On the domain  $S = 0, V_R > 0, V_L > 0$  and  $t \in [0, T], C(S, V_R, V_L, t) = 0$ .

- The terminal condition for the European call value is:

$$C(S, V_R, V_L, T) = (S - K)^+, \quad S \in \mathbb{R}, V_R > 0, V_L > 0$$

- **Boundary conditions on  $S$**

**Down and Out Calls.** On the domain  $S < L, V_R > 0, V_L > 0$  and  $t \in [0, T], C(S, V_R, V_L, t) = 0$ . We impose a zero gamma boundary condition at extremely high return levels:

$$\lim_{S \uparrow \infty} \frac{\partial^2}{\partial S^2} C(S, V_R, V_L, t) = 0, \quad V_R > 0, V_L > 0, t \in [0, T].$$

**Up and Out Calls.** On the domain  $H < S, V_R > 0, V_L > 0$  and  $t \in [0, T], C(S, V_R, V_L, t) = 0$ . On the domain  $S = 0, V_R > 0, V_L > 0$  and  $t \in [0, T], C(S, V_R, V_L, t) = 0$ .

**Double barrier Calls.** On the domain  $S < L, V_R > 0, V_L > 0$  or  $S < L, V_R > 0, V_L > 0$  and  $t \in [0, T], C(S, V_R, V_L, t) = 0$ .

## Boundary conditions on $V_R, V_L$

- There exist various opinions how to impose boundary conditions at extreme values of the activities (Tavella and Randall, 2000; Kluge 2002; Duffy 2004 and discussion at <http://www.wilmott.com>). We impose a Neumann-wise condition:

$$\lim_{V_R \uparrow \infty} \frac{\partial^2}{\partial S^2} C(S, V_R, V_L, t) = 0, \quad \lim_{V_L \uparrow \infty} \frac{\partial^2}{\partial S^2} C(S, V_R, V_L, t) = 0$$



## Boundary conditions on $V_R, V_L$

- There exist various opinions how to impose boundary conditions at extreme values of the activities (Tavella and Randall, 2000; Kluge 2002; Duffy 2004 and discussion at <http://www.wilmott.com>). We impose a Neumann-wise condition:

$$\lim_{V_R \uparrow \infty} \frac{\partial^2}{\partial S^2} C(S, V_R, V_L, t) = 0, \quad \lim_{V_L \uparrow \infty} \frac{\partial^2}{\partial S^2} C(S, V_R, V_L, t) = 0$$

These conditions mean that the diffusion flow vanishes at the boundary in the direction orthogonal to that boundary. We don't use these conditions as it is, instead substituting them into the PIDE and further use the obtained equation as the boundary condition.

## Boundary conditions on $V_R, V_L$

- There exist various opinions how to impose boundary conditions at extreme values of the activities (Tavella and Randall, 2000; Kluge 2002; Duffy 2004 and discussion at <http://www.wilmott.com>). We impose a Neumann-wise condition:

$$\lim_{V_R \uparrow \infty} \frac{\partial^2}{\partial S^2} C(S, V_R, V_L, t) = 0, \quad \lim_{V_L \uparrow \infty} \frac{\partial^2}{\partial S^2} C(S, V_R, V_L, t) = 0$$

These conditions mean that the diffusion flow vanishes at the boundary in the direction orthogonal to that boundary. We don't use these conditions as it is, instead substituting them into the PIDE and further use the obtained equation as the boundary condition.

- As either activity rate approaches zero, we must either evaluate the above PIDE with the appropriate value of  $V = 0$ , or else study the effect of reflecting boundary conditions. Some authors assume it is empirically safe to set  $V_{min} = 0$  and let the value of  $C$  vanish at  $V_{min}$ . However, such boundary conditions are inconsistent with the terminal function at  $t = T$  and  $S > K$ . This creates a jump in the option value at  $t = T$  and  $S > K$ .

# Boundary Conditions (Continued)

## Boundary conditions on $V_R, V_L$

- There exist various opinions how to impose boundary conditions at extreme values of the activities (Tavella and Randall, 2000; Kluge 2002; Duffy 2004 and discussion at <http://www.wilmott.com>). We impose a Neumann-wise condition:

$$\lim_{V_R \uparrow \infty} \frac{\partial^2}{\partial S^2} C(S, V_R, V_L, t) = 0, \quad \lim_{V_R \uparrow 0} \frac{\partial^2}{\partial S^2} C(S, V_R, V_L, t) = 0, \quad \lim_{V_L \uparrow \infty} \frac{\partial^2}{\partial S^2} C(S, V_R, V_L, t) = 0$$

These conditions mean that the diffusion flow vanishes at the boundary in the direction orthogonal to that boundary. We don't use these conditions as it is, instead substituting them into the PIDE and further use the obtained equation as the boundary condition.

- As either activity rate approaches zero, we must either evaluate the above PIDE with the appropriate value of  $V = 0$ , or else study the effect of reflecting boundary conditions. Some authors assume it is empirically safe to set  $V_{min} = 0$  and let the value of  $C$  vanish at  $V_{min}$ . However, such boundary conditions are inconsistent with the terminal function at  $t = T$  and  $S > K$ . This creates a jump in the option value at  $t = T$  and  $S > K$ . So

To obtain the European barrier option price under the SSM model we have to solve 3D unsteady PIDE.

**So far nobody faced this problem in math finance!**

# Some useful theorems

**Lemma 1.0.** *Matrix of second derivatives of the PIDE is positive definite if  $|\rho_L| < 1$  and  $|\rho_R| < 1$ .*

**Proof 1.0.** *Necessary and sufficient conditions for the matrix of coefficients  $(a_{ij})_{3 \times 3}$  to be positive definite are:*

$$\begin{aligned} a_{11}a_{22} - a_{12}^2 &> 0, & a_{11}a_{33} - a_{13}^2 &> 0, & a_{22}a_{33} - a_{23}^2 &> 0, \\ a_{11}a_{22}a_{33} - a_{11}a_{23}^2 - a_{22}a_{13}^2 - a_{33}a_{12}^2 + 2a_{12}a_{13}a_{23} &> 0 \end{aligned} \quad (18)$$

*These results are well known and follow from completion of squares. The proof is given in Fraser, Duncan and Collar, 1963.*

*For the PIDE and vector of independent variables  $\mathbf{x} = (x, v_r, v_l)$  the matrix  $(a_{ij})_{3 \times 3} \equiv a(\mathbf{x})$  is*

$$a(\mathbf{x}) = \frac{1}{2} \begin{vmatrix} \sigma^2 S^2 (V_L + V_R) & SV_R \sigma \sigma_V \rho_R & SV_L \sigma \sigma_V \rho_L \\ SV_R \sigma \sigma_V \rho_R & \sigma_V^2 V_R & 0 \\ SV_L \sigma \sigma_V \rho_L & 0 & \sigma_V^2 V_L \end{vmatrix} \quad (19)$$

To solve the PIDE we intend to utilize splitting (Yanenko 1971, Samarskii 1964, Dyakonov 1965). Marchuk 1975 and then Strang 1968 extended this idea for complex physical processes by providing in addition to splitting on spatial coordinates also splitting on physical processes.

Suppose we can write the PIDE in the form

$$\frac{\partial}{\partial \tau} C(S, V_R, V_L, \tau) = \sum_{i=1}^4 \mathcal{L}_i C(S, V_R, V_L, \tau). \quad (20)$$

We associate a Lie operator  $\mathcal{F}$  with each given operator  $\mathcal{L}$ . This Lie operator is a linear operator acting on the space of operators defined on  $\mathbf{S}$ . Operator  $\mathcal{F}$  maps each operator  $G$  into the new operator  $\mathcal{F}G$ , such that for any element  $c \in \mathbf{S}$

$$(\mathcal{F}G)(C) = G'(C)\mathcal{L}(C)$$

For the solution  $C(\tau)$  of the PIDE it easily follows that

$$(\mathcal{F}G)(C(\tau)) = \frac{\partial}{\partial \tau} G(C(\tau)), \quad (\mathcal{F}^k G)(C(\tau)) = \frac{\partial^k}{\partial \tau^k} G(C(\tau)).$$

## The Lie operator formalism - Cont'd

The above relations hold for any  $G$  defined on  $\mathbf{S}$ , in particular for the identity  $I$ . Inserting  $I$  for  $G$  and using the Taylor expansion of the true solution, we can write  $C(\tau + \theta)$  in terms of the exponentiated Lie operator form or Lie-Taylor series,

$$C(\tau + \theta) = (e^{\theta \mathcal{F}} I)(C(\tau)).$$



The above relations hold for any  $G$  defined on  $\mathbf{S}$ , in particular for the identity  $I$ . Inserting  $I$  for  $G$  and using the Taylor expansion of the true solution, we can write  $C(\tau + \theta)$  in terms of the exponentiated Lie operator form or Lie-Taylor series,

$$C(\tau + \theta) = (e^{\theta \mathcal{F}} I)(C(\tau)).$$

Then we compose the resulting exponentiated Lie operators in the same order as the solution operators in the splitting procedure, with which they are associated. For instance, the Strang splitting solution can be expressed as

$$\tilde{C}(\tau + \theta) = \left( e^{\frac{1}{2}\theta \mathcal{F}_1} e^{\frac{1}{2}\theta \mathcal{F}_2} e^{\theta \mathcal{F}_3} e^{\frac{1}{2}\theta \mathcal{F}_2} e^{\frac{1}{2}\theta \mathcal{F}_1} I \right) (\tilde{C}(\tau)). \quad (23)$$

The above relations hold for any  $G$  defined on  $\mathbf{S}$ , in particular for the identity  $I$ . Inserting  $I$  for  $G$  and using the Taylor expansion of the true solution, we can write  $C(\tau + \theta)$  in terms of the exponentiated Lie operator form or Lie-Taylor series,

$$C(\tau + \theta) = (e^{\theta \mathcal{F}} I)(C(\tau)).$$

Then we compose the resulting exponentiated Lie operators in the same order as the solution operators in the splitting procedure, with which they are associated. For instance, the Strang splitting solution can be expressed as

$$\tilde{C}(\tau + \theta) = \left( e^{\frac{1}{2}\theta \mathcal{F}_1} e^{\frac{1}{2}\theta \mathcal{F}_2} e^{\theta \mathcal{F}_3} e^{\frac{1}{2}\theta \mathcal{F}_2} e^{\frac{1}{2}\theta \mathcal{F}_1} I \right) (\tilde{C}(\tau)). \quad (25)$$

All we need now is the BCH formula that the product  $e^X e^Y$  can be written as the exponential  $e^Z$  of

$$Z = X + Y + \frac{1}{2}[X, Y] + \frac{1}{12}([X, X, Y] + [Y, Y, X]) + \frac{1}{24}[X, Y, Y, X] + \dots \quad (26)$$

The above relations hold for any  $G$  defined on  $\mathbf{S}$ , in particular for the identity  $I$ . Inserting  $I$  for  $G$  and using the Taylor expansion of the true solution, we can write  $C(\tau + \theta)$  in terms of the exponentiated Lie operator form or Lie-Taylor series,

$$C(\tau + \theta) = (e^{\theta \mathcal{F}} I)(C(\tau)).$$

Then we compose the resulting exponentiated Lie operators in the same order as the solution operators in the splitting procedure, with which they are associated. For instance, the Strang splitting solution can be expressed as

$$\tilde{C}(\tau + \theta) = \left( e^{\frac{1}{2}\theta \mathcal{F}_1} e^{\frac{1}{2}\theta \mathcal{F}_2} e^{\theta \mathcal{F}_3} e^{\frac{1}{2}\theta \mathcal{F}_2} e^{\frac{1}{2}\theta \mathcal{F}_1} I \right) (\tilde{C}(\tau)). \quad (27)$$

All we need now is the BCH formula that the product  $e^X e^Y$  can be written as the exponential  $e^Z$  of

$$Z = X + Y + \frac{1}{2}[X, Y] + \frac{1}{12}([X, X, Y] + [Y, Y, X]) + \frac{1}{24}[X, Y, Y, X] + \dots \quad (28)$$

## Our method - the main idea

First rewrite the PIDE in new variables  $x = \ln S/Q$ ,  $\tau = T - t$ , where  $Q$  is a certain constant. That gives

$$\begin{aligned}
 \frac{\partial}{\partial \tau} C &= -r_d C(x, V_R, V_L, \tau) + \left[ r_d - r_f - \frac{\sigma^2}{2} (V_L + V_R) - a_R \sqrt{V_R} - a_L \sqrt{V_L} \right] \frac{\partial}{\partial x} C \\
 &+ \kappa(1 - V_R) \frac{\partial}{\partial V_R} C + \kappa(1 - V_L) \frac{\partial}{\partial V_L} C + \frac{\sigma^2 (V_R + V_L)}{2} \frac{\partial^2}{\partial x^2} C + \sigma \rho^R \sigma_V V_R \frac{\partial^2}{\partial x \partial V_R} C \\
 &+ \sigma \rho^L \sigma_V V_L \frac{\partial^2}{\partial x \partial V_L} C + \frac{\sigma_V^2 V_R}{2} \frac{\partial^2}{\partial V_R^2} C + \frac{\sigma_V^2 V_L}{2} \frac{\partial^2}{\partial V_L^2} C \\
 &+ \sqrt{V_R} \int_0^\infty \left[ C(x + y, V_R, V_L, \tau) - C - y \frac{\partial}{\partial x} C \right] \lambda \frac{e^{-|y|/\nu_j}}{|y|^{1+\alpha}} dy \\
 &+ \sqrt{V_L} \int_{-\infty}^0 \left[ C(x + y, V_R, V_L, \tau) - C - y \frac{\partial}{\partial x} C \right] \lambda \frac{e^{-|y|/\nu_j}}{|y|^{1+\alpha}} dy,
 \end{aligned} \tag{28}$$

where

$$\begin{aligned}
 a_R &= \int_0^\infty (e^y - 1 - y) \lambda \frac{e^{-|y|/\nu_j}}{|y|^{1+\alpha}} dy \\
 a_L &= \int_{-\infty}^0 (e^y - 1 - y) \lambda \frac{e^{-|y|/\nu_j}}{|y|^{1+\alpha}} dy
 \end{aligned}$$

## Main idea (Continued)

Now we represent the above equation in the form

$$\frac{\partial}{\partial \tau} C(x, V_R, V_L, \tau) = (L_1 + L_2)C(x, V_R, V_L, \tau), \quad (30)$$

where

$$\begin{aligned} L_i C &= -\frac{1}{2}r_d C + \left( \frac{1}{2}(r_d - r_f) - \frac{1}{2}\sigma^2 V_i - a_i \sqrt{V_i} \right) \frac{\partial}{\partial x} C \\ &+ \kappa(1 - V_i) \frac{\partial}{\partial V_i} C + \frac{\sigma^2 V_i}{2} \frac{\partial^2}{\partial x^2} C + \sigma \rho_i \sigma_V V_i \frac{\partial^2}{\partial x \partial V_i} C \\ &+ \frac{\sigma_V^2 V_i}{2} \frac{\partial^2}{\partial V_i^2} C + \sqrt{V_i} \int_i \left[ C(x + y, V_R, V_L, \tau) - C - y \frac{\partial}{\partial x} C \right] \lambda \frac{e^{-|y|/\nu_j}}{|y|^{1+\alpha}} dy, \end{aligned} \quad (31)$$

and  $i = R, L$  and  $\int_R = \int_0^\infty, \int_L = \int_{-\infty}^0$ .

## Main idea (Continued)

Now we represent the above equation in the form

$$\frac{\partial}{\partial \tau} C(x, V_R, V_L, \tau) = (L_1 + L_2)C(x, V_R, V_L, \tau), \quad (31)$$

where

$$\begin{aligned} L_i C &= -\frac{1}{2}r_d C + \left( \frac{1}{2}(r_d - r_f) - \frac{1}{2}\sigma^2 V_i - a_i \sqrt{V_i} \right) \frac{\partial}{\partial x} C \\ &+ \kappa(1 - V_i) \frac{\partial}{\partial V_i} C + \frac{\sigma^2 V_i}{2} \frac{\partial^2}{\partial x^2} C + \sigma \rho_i \sigma_V V_i \frac{\partial^2}{\partial x \partial V_i} C \\ &+ \frac{\sigma_V^2 V_i}{2} \frac{\partial^2}{\partial V_i^2} C + \sqrt{V_i} \int_i \left[ C(x + y, V_R, V_L, \tau) - C - y \frac{\partial}{\partial x} C \right] \lambda \frac{e^{-|y|/\nu_j}}{|y|^{1+\alpha}} dy, \end{aligned} \quad (32)$$

and  $i = R, L$  and  $\int_R = \int_0^\infty$ ,  $\int_L = \int_{-\infty}^0$ .

**Lemma 1.1.**

$$[L_R, L_L] = 0$$

## Main idea (Continued)

Now we represent the above equation in the form

$$\frac{\partial}{\partial \tau} C(x, V_R, V_L, \tau) = (L_1 + L_2)C(x, V_R, V_L, \tau), \quad (33)$$

where

$$\begin{aligned} L_i C &= -\frac{1}{2}r_d C + \left( \frac{1}{2}(r_d - r_f) - \frac{1}{2}\sigma^2 V_i - a_i \sqrt{V_i} \right) \frac{\partial}{\partial x} C \\ &+ \kappa(1 - V_i) \frac{\partial}{\partial V_i} C + \frac{\sigma^2 V_i}{2} \frac{\partial^2}{\partial x^2} C + \sigma \rho_i \sigma_V V_i \frac{\partial^2}{\partial x \partial V_i} C \\ &+ \frac{\sigma_V^2 V_i}{2} \frac{\partial^2}{\partial V_i^2} C + \sqrt{V_i} \int_i \left[ C(x + y, V_R, V_L, \tau) - C - y \frac{\partial}{\partial x} C \right] \lambda \frac{e^{-|y|/\nu_j}}{|y|^{1+\alpha}} dy, \end{aligned} \quad (34)$$

and  $i = R, L$  and  $\int_R = \int_0^\infty$ ,  $\int_L = \int_{-\infty}^0$ .

**Lemma 1.1.**

$$[L_R, L_L] = 0$$

**Proof 1.1.** *Without the integral terms it could be easily verified with Mathematica. The integral terms could be expanded into power series on  $y$ . All coefficients of  $I_R$  are just functions of  $V_R$ , and all coefficients of  $I_L$  are just functions of  $V_L$ . Therefore,  $I_R$  commutes with  $I_L$  and the diffusion part of  $L_L$ . And vice versa.*

## Main idea (Continued)

Now we represent the above equation in the form

$$\frac{\partial}{\partial \tau} C(x, V_R, V_L, \tau) = (L_1 + L_2)C(x, V_R, V_L, \tau), \quad (35)$$

where

$$\begin{aligned} L_i C &= -\frac{1}{2}r_d C + \left( \frac{1}{2}(r_d - r_f) - \frac{1}{2}\sigma^2 V_i - a_i \sqrt{V_i} \right) \frac{\partial}{\partial x} C \\ &+ \kappa(1 - V_i) \frac{\partial}{\partial V_i} C + \frac{\sigma^2 V_i}{2} \frac{\partial^2}{\partial x^2} C + \sigma \rho_i \sigma_V V_i \frac{\partial^2}{\partial x \partial V_i} C \\ &+ \frac{\sigma_V^2 V_i}{2} \frac{\partial^2}{\partial V_i^2} C + \sqrt{V_i} \int_i \left[ C(x + y, V_R, V_L, \tau) - C - y \frac{\partial}{\partial x} C \right] \lambda \frac{e^{-|y|/\nu_j}}{|y|^{1+\alpha}} dy, \end{aligned} \quad (36)$$

and  $i = R, L$  and  $\int_R = \int_0^\infty$ ,  $\int_L = \int_{-\infty}^0$ .

**Lemma 1.1.**

$$[L_R, L_L] = 0$$

**Proof 1.1.** Without the integral terms it could be easily verified with *Mathematica*. The integral terms could be expanded into power series on  $y$ . All coefficients of  $I_R$  are just functions of  $V_R$ , and all coefficients of  $I_L$  are just functions of  $V_L$ . Therefore,  $I_R$  commutes with  $I_L$  and the diffusion part of  $L_L$ . And vice versa.



## Jump-diffusion splitting

- The idea of splitting on physical processes for jump-diffusion models has been already proposed by Cont and Volchkova. They split the operator  $L$  into two parts:

$$\frac{\partial}{\partial \tau} C(S, V_R, V_L, \tau) = \mathcal{D}C(S, V_R, V_L, \tau) + \mathcal{J}C(S, V_R, V_L, \tau), \quad (38)$$

where  $\mathcal{D}$  and  $\mathcal{J}$  stand for the differential and integral parts of  $L$  respectively.

- The idea of splitting on physical processes for jump-diffusion models has been already proposed by Cont and Volchkova. They split the operator  $L$  into two parts:

$$\frac{\partial}{\partial \tau} C(S, V_R, V_L, \tau) = \mathcal{D}C(S, V_R, V_L, \tau) + \mathcal{J}C(S, V_R, V_L, \tau), \quad (39)$$

where  $\mathcal{D}$  and  $\mathcal{J}$  stand for the differential and integral parts of  $L$  respectively.

- They replace  $\mathcal{D}C$  with a FD approximation  $D$ ,  $\mathcal{J}C$  with a certain finite approximation of the integral  $J$  (that we will further discuss) and use the following explicit-implicit time stepping scheme:

$$\frac{C^{n+1} - C^n}{\Delta \tau} = DC^{n+1} + JC^n \quad (40)$$

- The idea of splitting on physical processes for jump-diffusion models has been already proposed by Cont and Volchkova. They split the operator  $L$  into two parts:

$$\frac{\partial}{\partial \tau} C(S, V_R, V_L, \tau) = \mathcal{D}C(S, V_R, V_L, \tau) + \mathcal{J}C(S, V_R, V_L, \tau), \quad (41)$$

where  $\mathcal{D}$  and  $\mathcal{J}$  stand for the differential and integral parts of  $L$  respectively.

- They replace  $\mathcal{D}C$  with a FD approximation  $D$ ,  $\mathcal{J}C$  with a certain finite approximation of the integral  $J$  (that we will further discuss) and use the following explicit-implicit time stepping scheme:

$$\frac{C^{n+1} - C^n}{\Delta \tau} = DC^{n+1} + JC^n \quad (42)$$

- Thus, Cont and Volchkova treat the integral part explicitly to avoid the inversion of the non-sparse matrix  $J$ . They show that this does not affect the stability of the scheme: it remains unconditionally stable.

## Order of approximation!

- Unfortunately this scheme approximates the original PIDE with the accuracy  $O(\theta)$ . The higher-order operator splitting algorithms can be obtained, for instance, by doing one time step of the Strang splitting method, which consists of three substeps:

$$\begin{aligned}\frac{C(S, V_R, V_L, \tau)^* - C(S, V_R, V_L, \tau)^n}{\Delta\tau/2} &= DC(S, V_R, V_L, \tau)^* \\ \frac{C(S, V_R, V_L, \tau)^{**} - C(S, V_R, V_L, \tau)^*}{\Delta\tau} &= JC(S, V_R, V_L, \tau)^* \\ \frac{C(S, V_R, V_L, \tau)^{n+1} - C(S, V_R, V_L, \tau)^{**}}{\Delta\tau/2} &= DC(S, V_R, V_L, \tau)^{n+1}\end{aligned}$$

## Order of approximation!

- Unfortunately this scheme approximates the original PIDE with the accuracy  $O(\theta)$ . The higher-order operator splitting algorithms can be obtained, for instance, by doing one time step of the Strang splitting method, which consists of three substeps:

$$\begin{aligned}\frac{C(S, V_R, V_L, \tau)^* - C(S, V_R, V_L, \tau)^n}{\Delta\tau/2} &= DC(S, V_R, V_L, \tau)^* \\ \frac{C(S, V_R, V_L, \tau)^{**} - C(S, V_R, V_L, \tau)^*}{\Delta\tau} &= JC(S, V_R, V_L, \tau)^* \\ \frac{C(S, V_R, V_L, \tau)^{n+1} - C(S, V_R, V_L, \tau)^{**}}{\Delta\tau/2} &= DC(S, V_R, V_L, \tau)^{n+1}\end{aligned}$$

- Usually for parabolic equations with constant coefficients this composite algorithm is second-order-accurate provided the numerical procedures for the split equations are at least second-order-accurate.

## Order of approximation!

- Unfortunately this scheme approximates the original PIDE with the accuracy  $O(\theta)$ . The higher-order operator splitting algorithms can be obtained, for instance, by doing one time step of the Strang splitting method, which consists of three substeps:

$$\begin{aligned}\frac{C(S, V_R, V_L, \tau)^* - C(S, V_R, V_L, \tau)^n}{\Delta\tau/2} &= DC(S, V_R, V_L, \tau)^* \\ \frac{C(S, V_R, V_L, \tau)^{**} - C(S, V_R, V_L, \tau)^*}{\Delta\tau} &= JC(S, V_R, V_L, \tau)^* \\ \frac{C(S, V_R, V_L, \tau)^{n+1} - C(S, V_R, V_L, \tau)^{**}}{\Delta\tau/2} &= DC(S, V_R, V_L, \tau)^{n+1}\end{aligned}$$

- Usually for parabolic equations with constant coefficients this composite algorithm is second-order-accurate provided the numerical procedures for the split equations are at least second-order-accurate.
- The parabolic part exactly coincides with the Heston model!

# Numerical method

## Reasons

- FD methods often require equal grid steps in  $S$  and  $V_R, V_L$  domains, so to achieve that the original independent variables should be normalized.



## Reasons

- FD methods often require equal grid steps in  $S$  and  $V_R, V_L$  domains, so to achieve that the original independent variables should be normalized.
- The solution of the PIDE is very sensitive to localization errors when  $S$  is in the vicinity of  $K$ . To increase accuracy it would be reasonable to use an adaptive mesh with high concentration of the mesh points around  $S = K$ .

## Reasons

- FD methods often require equal grid steps in  $S$  and  $V_R, V_L$  domains, so to achieve that the original independent variables should be normalized.
- The solution of the PIDE is very sensitive to localization errors when  $S$  is in the vicinity of  $K$ . To increase accuracy it would be reasonable to use an adaptive mesh with high concentration of the mesh points around  $S = K$ .
- For the barrier options the situation is even more complicated. Here we consider only continuously sampled barriers, so it is sufficient to place the barriers on the boundaries of the grid and enforce a boundary condition of zero option value. The gradient of the option price is discontinuous at the barriers because we never solve the pricing equation (which includes second derivative terms that might become singular) there. So we need an adaptive grid as well.

# Coordinate transformation (Cont'd)

Let us use a map  $S \leftrightarrow x, V_R \leftrightarrow v_r, V_L \leftrightarrow v_l, t \leftrightarrow \tau$  of the form

$$S = S(x), \quad v_r = V_R(v_r), \quad v_l = V_L(v_l), \quad \tau = T - t. \quad (47)$$

# Coordinate transformation (Cont'd)

Let us use a map  $S \leftrightarrow x, V_R \leftrightarrow v_r, V_L \leftrightarrow v_l, t \leftrightarrow \tau$  of the form

$$S = S(x), \quad v_r = V_R(v_r), \quad v_l = V_L(v_l), \quad \tau = T - t. \quad (49)$$

Tavella, Randall 2000 define the Jacobian of this transformation

$$J(x) = dS(x)/dx, \quad (50)$$

as

$$J(x) = A \left[ \sum_{k=1}^{k=3} J_k(x)^{-2} \right]^{-1/2}, \quad J_k(x) = [\alpha_k^2 + (S(x) - B_k)^2]^{1/2}$$

Parameters  $B_k$  correspond to the critical points, i.e. in our case

$B_1 \equiv \mathcal{L}, B_2 \equiv \mathcal{H}, B_3 \equiv K, \mathcal{H} = \min(H, S_{max}), \mathcal{L} = \max(L, S_{min})$ . Parameters  $A$  and  $\alpha_k, k = 1, 2, 3$  are adjustable. Setting  $\alpha_k \ll \mathcal{H} - \mathcal{L}$  yields a highly nonuniform grid while  $\alpha_k \gg \mathcal{H} - \mathcal{L}$  yields a uniform grid.

# Coordinate transformation (Cont'd)

Let us use a map  $S \leftrightarrow x, V_R \leftrightarrow v_r, V_L \leftrightarrow v_l, t \leftrightarrow \tau$  of the form

$$S = S(x), \quad v_r = V_R(v_r), \quad v_l = V_L(v_l), \quad \tau = T - t. \quad (52)$$

Tavella, Randall 2000 define the Jacobian of this transformation

$$J(x) = dS(x)/dx, \quad (53)$$

as

$$J(x) = A \left[ \sum_{k=1}^{k=3} J_k(x)^{-2} \right]^{-1/2}, \quad J_k(x) = [\alpha_k^2 + (S(x) - B_k)^2]^{1/2}$$

Parameters  $B_k$  correspond to the critical points, i.e. in our case

$B_1 \equiv \mathcal{L}, B_2 \equiv \mathcal{H}, B_3 \equiv K, \mathcal{H} = \min(H, S_{max}), \mathcal{L} = \max(L, S_{min})$ . Parameters  $A$  and  $\alpha_k, k = 1, 2, 3$  are adjustable. Setting  $\alpha_k \ll \mathcal{H} - \mathcal{L}$  yields a highly nonuniform grid while  $\alpha_k \gg \mathcal{H} - \mathcal{L}$  yields a uniform grid.

To obey the boundary condition  $S(1) = \mathcal{H}$  one can vary  $A$ . Since  $S(x = 1)$  is monotonically increasing with  $A$  the numerical iterations are guaranteed to converge.

# Coordinate transformation - results

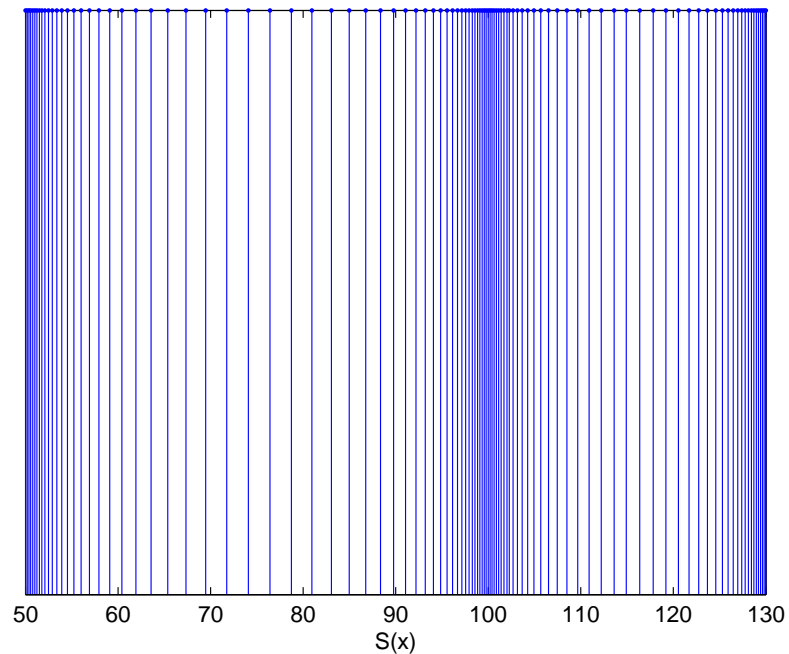


Figure 1: New grid in  $x$  that contains 100 nodes uniformly distributed from 0 to 1. Value of parameters used in this example are:  $H = 130, L = 50, K = 100, \alpha_H = \alpha_L = (H - L)/60, \alpha_K = (H - K)/20$ . The computed value of  $A$  is 13.935.

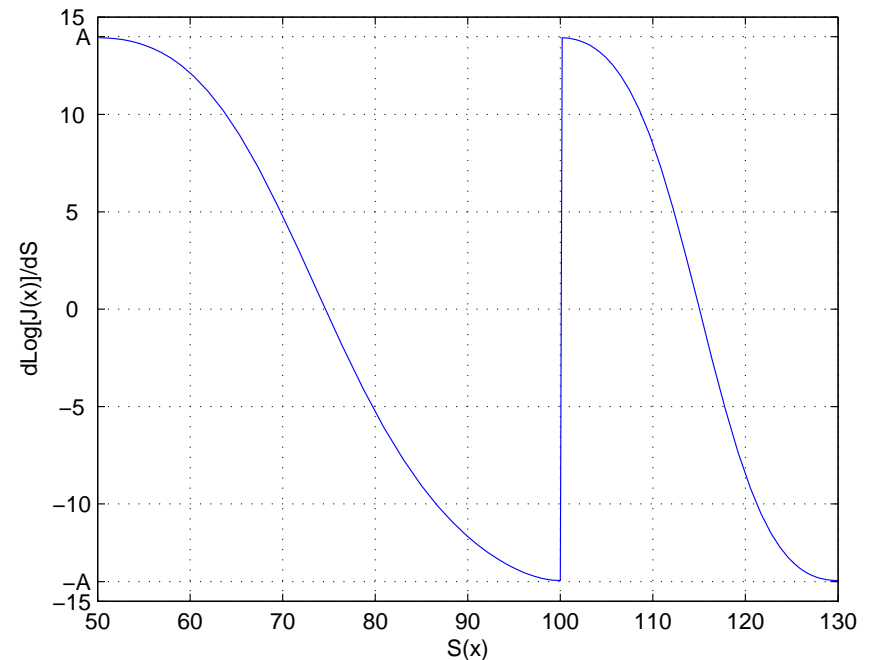
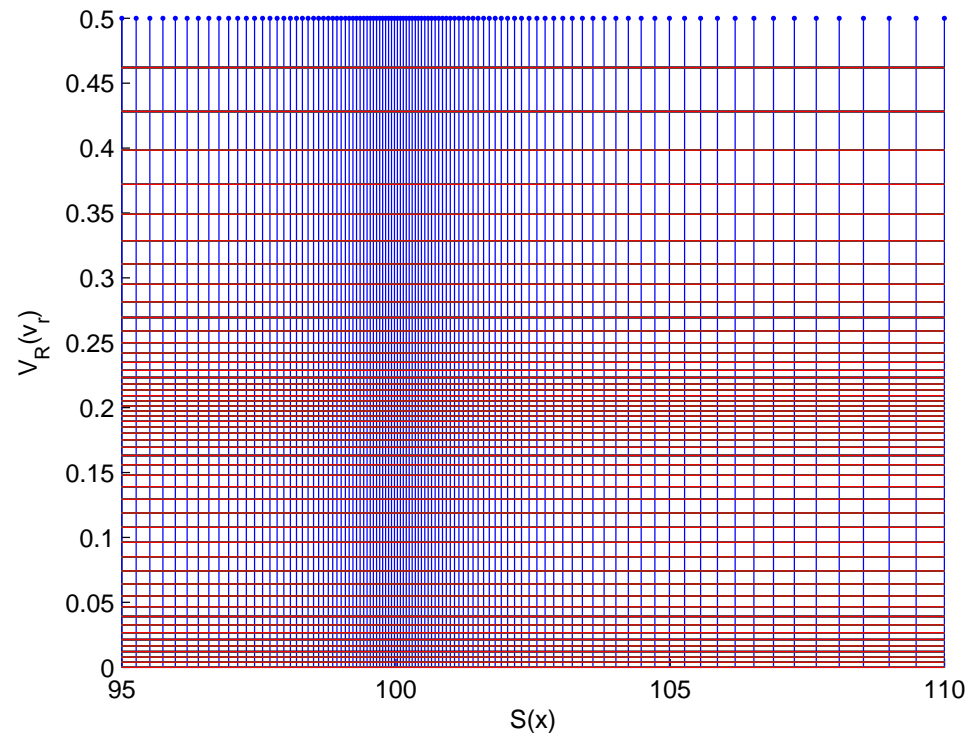


Figure 2:  $d \ln J(x)/dx$  as a function of  $S(x)$ . Parameters for this test are same

# Coordinate transformation - results 2

In this Fig. we present a map of the new grid obtained from the original uniform  $S - V_R$  grid by using the above transformation. The new grid contains 100 nodes in  $x$  uniformly distributed from 0 to 1, and 100 nodes in  $v_r$  also uniformly distributed from 0 to 1. Value of parameters used in this example are:  $H = 110, L = 95, K = 100, \alpha_H = \alpha_L = (H - L)/0.1, \alpha_K = (H - K)/10, \alpha_0 = \alpha_{v_0} = V_{max}/20$ , where  $V_{max}$  is a maximum value of  $V_R$  and  $V_L$  on the grid (here  $V_{max} = 0.5$ ), and  $v_0 = 0.2$ .



# Jumps with a finite activity

Every term under the integral exists, and therefore two last terms could be integrated out. If  $W = W(S(x), v_r, v_l, \tau)$ , then

$$\int_i \left[ W(S(x)e^y) - W(S(x), v_r, v_l, \tau) - \xi(x) \frac{\partial}{\partial x} W(e^y - 1) \right] \lambda \frac{e^{-|y|/\nu_j}}{|y|^{1+\alpha}} dy =$$
$$\int_i W(S(x)e^y) \mu(dy) - \beta_i \xi(x) \frac{\partial}{\partial x} W - \gamma_i W,$$
$$\beta_i = \int_i (e^y - 1) \mu(dy), \quad \gamma_i = \int_i \mu(dy), \quad \mu(dy) = \lambda \frac{e^{-|y|/\nu_j}}{|y|^{1+\alpha}} dy.$$

where  $\xi(x) \equiv S(x)/J(x)$ ,  $\eta_r(v_r) \equiv V_R/J_r(v_r)$ ,  $\eta_l(v_l) \equiv V_L/J_l(v_l)$ , Jacobians  $J_r(v_r)$  and  $J_l(v_l)$  are defined as  $J_r(v_r) = dV_R(v_r)/dv_r$ ,  $J_l(v_l) = dV_L(v_l)/dv_l$ .

In our setup  $\beta_i$  and  $\gamma_i$  are constants that can be precomputed!



# Jumps with a finite activity

Every term under the integral exists, and therefore two last terms could be integrated out. If  $W = W(S(x), v_r, v_l, \tau)$ , then

$$\int_i \left[ W(S(x)e^y) - W(S(x), v_r, v_l, \tau) - \xi(x) \frac{\partial}{\partial x} W(e^y - 1) \right] \lambda \frac{e^{-|y|/\nu_j}}{|y|^{1+\alpha}} dy =$$
$$\int_i W(S(x)e^y) \mu(dy) - \beta_i \xi(x) \frac{\partial}{\partial x} W - \gamma_i W,$$
$$\beta_i = \int_i (e^y - 1) \mu(dy), \quad \gamma_i = \int_i \mu(dy), \quad \mu(dy) = \lambda \frac{e^{-|y|/\nu_j}}{|y|^{1+\alpha}} dy.$$

where  $\xi(x) \equiv S(x)/J(x)$ ,  $\eta_r(v_r) \equiv V_R/J_r(v_r)$ ,  $\eta_l(v_l) \equiv V_L/J_l(v_l)$ , Jacobians  $J_r(v_r)$  and  $J_l(v_l)$  are defined as  $J_r(v_r) = dV_R(v_r)/dv_r$ ,  $J_l(v_l) = dV_L(v_l)/dv_l$ .

In our setup  $\beta_i$  and  $\gamma_i$  are constants that can be precomputed!

The first integral has to be computed with the second order approximation in  $x$  to preserve the second order approximation of the whole method. The trapezoidal approximation suffices for the second order but higher order methods are often even faster. Therefore, we use adaptive Lobatto quadratures.

# Jumps with a finite activity (Cont'd)

According to the above representation the 2d PIDE now reads

$$\frac{\partial}{\partial \tau} W(S(x), v_r, v_l, \tau) = L_{1d} W(S(x), v_r, v_l, \tau) + I(S(x), v_r, v_l, \tau)$$

$$I(S(x), v_r, v_l, \tau) = \int_i W(S(x)e^y, v_r, v_l, \tau) \lambda \frac{e^{-|y|/\nu_j}}{|y|^{1+\alpha}} dy$$

$$L_{1d} = k_0 + k_1 \frac{\partial}{\partial x} + k_2 \frac{\partial}{\partial v_i} + k_{11} \frac{\partial^2}{\partial x^2} + k_{12} \frac{\partial^2}{\partial x \partial v_i} + k_{22} \frac{\partial^2}{\partial v_i^2}$$

$$k_0 = -\frac{1}{2}r_d - \gamma_i \sqrt{V_i(v_i)}, \quad k_{11} = V_i(v_i) \frac{\sigma^2 \xi^2(x) J(x)}{2}, \quad k_{12} = \sigma \rho_i \sigma_V \xi(x) \eta_i(v_i),$$

$$k_1 = \left[ \frac{1}{2}(r_d - r_f) - \beta_i \sqrt{V_i(v_i)} \right] \xi(x) - \frac{1}{2} V_i(v_i) \sigma^2 \xi^2(x) \frac{d \ln J(x)}{dx}$$

$$k_2 = \frac{\kappa}{J_i} (1 - V_i(v_i)) - \frac{1}{2J_i} \sigma_V^2 \eta_i(v_i) \frac{d \ln J_i(v_i)}{dv_i}, \quad k_{22} = \frac{\sigma_V^2 \eta_i(v_i)}{2}$$

# Jumps with a finite activity (Cont'd)

According to the above representation the 2d PIDE now reads

$$\frac{\partial}{\partial \tau} W(S(x), v_r, v_l, \tau) = L_{1d} W(S(x), v_r, v_l, \tau) + I(S(x), v_r, v_l, \tau)$$

$$I(S(x), v_r, v_l, \tau) = \int_i W(S(x)e^y, v_r, v_l, \tau) \lambda \frac{e^{-|y|/\nu_j}}{|y|^{1+\alpha}} dy$$

$$L_{1d} = k_0 + k_1 \frac{\partial}{\partial x} + k_2 \frac{\partial}{\partial v_i} + k_{11} \frac{\partial^2}{\partial x^2} + k_{12} \frac{\partial^2}{\partial x \partial v_i} + k_{22} \frac{\partial^2}{\partial v_i^2}$$

$$k_0 = -\frac{1}{2}r_d - \gamma_i \sqrt{V_i(v_i)}, \quad k_{11} = V_i(v_i) \frac{\sigma^2 \xi^2(x) J(x)}{2}, \quad k_{12} = \sigma \rho_i \sigma_V \xi(x) \eta_i(v_i),$$

$$k_1 = \left[ \frac{1}{2}(r_d - r_f) - \beta_i \sqrt{V_i(v_i)} \right] \xi(x) - \frac{1}{2} V_i(v_i) \sigma^2 \xi^2(x) \frac{d \ln J(x)}{dx}$$

$$k_2 = \frac{\kappa}{J_i} (1 - V_i(v_i)) - \frac{1}{2J_i} \sigma_V^2 \eta_i(v_i) \frac{d \ln J_i(v_i)}{dv_i}, \quad k_{22} = \frac{\sigma_V^2 \eta_i(v_i)}{2}$$

- As one of the limits of our integrals is infinite it has to be truncated to reduce the region of integration to a bounded interval. For options with the existing upper barrier, in the integral  $\int_0^\infty$  the upper limit can be truncated to  $\mathcal{H}$ . This amounts to the truncation of large jumps. For the detailed discussion of this issue see Cont, Volchkova 2003.

# Jumps with a finite activity (Cont'd)

- Now let us introduce a grid in  $y - y_i$ ,  $i = 1 \dots N$ . If this grid is uniform or adaptive in general it doesn't coincide with the grid in variable  $x$  or  $S(x)$ . Therefore, to find the value of  $Z(S(x)e^{y_i}, v_r, v_l, \tau)$  at least linear interpolation has to be used at each point  $i = 1, \dots, N$  to preserve second order of approximation. Under this procedure, one has to check if the value  $S(x)e^{y_i}$  belongs to the computational domain on  $x$ . Otherwise, the value of  $Z$  is set to the corresponding boundary value. For instance, in case of a double barrier option it must vanish outside the barriers.

# Jumps with a finite activity (Cont'd)

- Now let us introduce a grid in  $y - y_i$ ,  $i = 1 \dots N$ . If this grid is uniform or adaptive in general it doesn't coincide with the grid in variable  $x$  or  $S(x)$ . Therefore, to find the value of  $Z(S(x)e^{y_i}, v_r, v_l, \tau)$  at least linear interpolation has to be used at each point  $i = 1, \dots, N$  to preserve second order of approximation. Under this procedure, one has to check if the value  $S(x)e^{y_i}$  belongs to the computational domain on  $x$ . Otherwise, the value of  $Z$  is set to the corresponding boundary value. For instance, in case of a double barrier option it must vanish outside the barriers.
- When the activity is infinite (for instance, the VG model) it is well-known that last two terms under the integral can not be integrated out, because they don't exist under such a kernel. Therefore, we must remain them under the integral and treat them as a part of the integral.

# Jumps with a finite activity (Cont'd)

- Now let us introduce a grid in  $y - y_i$ ,  $i = 1...N$ . If this grid is uniform or adaptive in general it doesn't coincide with the grid in variable  $x$  or  $S(x)$ . Therefore, to find the value of  $Z(S(x)e^{y_i}, v_r, v_l, \tau)$  at least linear interpolation has to be used at each point  $i = 1, \dots, N$  to preserve second order of approximation. Under this procedure, one has to check if the value  $S(x)e^{y_i}$  belongs to the computational domain on  $x$ . Otherwise, the value of  $Z$  is set to the corresponding boundary value. For instance, in case of a double barrier option it must vanish outside the barriers.
- When the activity is infinite (for instance, the VG model) it is well-known that last two terms under the integral can not be integrated out, because they don't exist under such a kernel. Therefore, we must remain them under the integral and treat them as a part of the integral.
- In our FD scheme we treat the integral as a source term using its value from the previous time step. In case of jumps of the finite activity we could integrate the second and third terms out and add them to the corresponding terms in the differential part, further applying the below described method.

- Crank-Nicholson scheme where approximation of the source term is made by using a one-side finite difference to preserve the second order approximation in time. Let  $W = W(x, v_r, v_l)$

$$\frac{W^{n+1} - W^n}{\theta} = \frac{1}{2}(L_{1d}W^{n+1} + L_{1d}W^n) + \frac{3}{2}I^n - \frac{1}{2}I^{n-1}.$$

- Crank-Nicholson scheme where approximation of the source term is made by using a one-side finite difference to preserve the second order approximation in time. Let  $W = W(x, v_r, v_l)$

$$\frac{W^{n+1} - W^n}{\theta} = \frac{1}{2}(L_{1d}W^{n+1} + L_{1d}W^n) + \frac{3}{2}I^n - \frac{1}{2}I^{n-1}.$$

- As the initial (terminal) condition is not sufficiently smooth, at first three steps we use a fully implicit Euler scheme

$$\frac{W^{n+1} - W^n}{\theta} = L_{1d}W^{n+1} + I^n$$

providing  $O(\theta)$  approximation. This increases stability of the whole scheme and often allows one to avoid oscillations inherent to the Crank-Nicholson method.



- Crank-Nicholson scheme where approximation of the source term is made by using a one-side finite difference to preserve the second order approximation in time. Let  $W = W(x, v_r, v_l)$

$$\frac{W^{n+1} - W^n}{\theta} = \frac{1}{2}(L_{1d}W^{n+1} + L_{1d}W^n) + \frac{3}{2}I^n - \frac{1}{2}I^{n-1}.$$

- As the initial (terminal) condition is not sufficiently smooth, at first three steps we use a fully implicit Euler scheme

$$\frac{W^{n+1} - W^n}{\theta} = L_{1d}W^{n+1} + I^n$$

providing  $O(\theta)$  approximation. This increases stability of the whole scheme and often allows one to avoid oscillations inherent to the Crank-Nicholson method.

- Alternative to the Crank-Nicholson scheme we also use the BDF2 scheme (see Hundsdorfer and Verwer)

$$W^{n+1} = \frac{4}{3}W^n - \frac{1}{3}W^{n-1} + \frac{2}{3}\theta L_{1d}W^{n+1} + \frac{2}{3}\theta [2I^n - I^{n-1}].$$

# Approximation of derivatives

■ We use standard second-order accurate central finite differences.

$$\delta_x W_{ij} = \frac{W_{i+1,j} - W_{i-1,j}}{h_1}, \quad \delta_v W_{ij} = \frac{W_{i,j-1} - W_{i,j+1}}{h_2} \quad (63)$$

$$\delta_x^2 W_{ij} = \frac{W_{i+1,j} - 2W_{i,j} + W_{i-1,j}}{h_1^2}, \quad \delta_v^2 W_{ij} = \frac{W_{i,j+1} - 2W_{i,j} + W_{i,j-1}}{h_2^2},$$

$$\delta_{xv}^2 W_{ij} = \frac{W_{i+1,j+1} - W_{i+1,j-1} - W_{i-1,j+1} + W_{i-1,j-1}}{4h_1h_2},$$

# Approximation of derivatives

■ We use standard second-order accurate central finite differences.

$$\delta_x W_{ij} = \frac{W_{i+1,j} - W_{i-1,j}}{h_1}, \quad \delta_v W_{ij} = \frac{W_{i,j-1} - W_{i,j+1}}{h_2} \quad (65)$$

$$\delta_x^2 W_{ij} = \frac{W_{i+1,j} - 2W_{i,j} + W_{i-1,j}}{h_1^2}, \quad \delta_v^2 W_{ij} = \frac{W_{i,j+1} - 2W_{i,j} + W_{i,j-1}}{h_2^2},$$

$$\delta_{xv}^2 W_{ij} = \frac{W_{i+1,j+1} - W_{i+1,j-1} - W_{i-1,j+1} + W_{i-1,j-1}}{4h_1h_2},$$

■ At  $j = 0$  and  $j = N_2$  we impose a Neumann-wise boundary condition approximated using the central finite difference operators

$$\delta_v^2 W_{i0} = \frac{W_{i+1,-1} - 2W_{i,0} + W_{i-1,1}}{h_1^2} = 0 \quad (65)$$

$$\delta_v^2 W_{iN} = \frac{W_{i+1,N+1} - 2W_{i,N} + W_{i-1,N-1}}{h_2^2} = 0$$

From this it follows that the fictitious grid point values  $W_{i,-1}$  and  $W_{i,N+1}$  that lies outside the computational domain could be expressed via the known grid point values. We can use this knowledge to eliminate all fictitious grid point values appearing in the stencil.

# FD equation

Therefore, for the internal points  $i = 1 \dots N_1 - 1, j = 1 \dots N_2 - 1$  we obtain the following scheme

$$\begin{aligned} L_{1d}(i, j) = & \left[ \frac{k_{12}}{4h_1h_2} W_{i-1, j-1} + \left( -\frac{k_1}{2h_1} + \frac{k_{11}}{h_1^2} \right) W_{i-1, j} - \frac{k_{12}}{4h_1h_2} W_{i-1, j+1} \right] \\ & \left[ \left( -\frac{k_2}{2h_2} + \frac{k_{22}}{h_2^2} \right) W_{i, j-1} + \left( -r_d - 2\frac{k_{11}}{h_1^2} - \frac{k_{22}}{h_2^2} \right) W_{i, j} + \left( \frac{k_2}{2h_2} + \frac{k_{22}}{h_2^2} \right) W_{i, j+1} \right] \\ & + \left[ -\frac{k_{12}}{4h_1h_2} W_{i+1, j-1} + \left( \frac{k_1}{2h_1} + \frac{k_{11}}{h_1^2} \right) W_{i+1, j} + \frac{k_{12}}{4h_1h_2} W_{i+1, j+1} \right] \\ & + O(h_1^2 + h_2^2 + h_1h_2) \end{aligned}$$

# FD equation

- Therefore, for the internal points  $i = 1 \dots N_1 - 1, j = 1 \dots N_2 - 1$  we obtain the following scheme

$$\begin{aligned} L_{1d}(i, j) = & \left[ \frac{k_{12}}{4h_1h_2} W_{i-1, j-1} + \left( -\frac{k_1}{2h_1} + \frac{k_{11}}{h_1^2} \right) W_{i-1, j} - \frac{k_{12}}{4h_1h_2} W_{i-1, j+1} \right] \\ & \left[ \left( -\frac{k_2}{2h_2} + \frac{k_{22}}{h_2^2} \right) W_{i, j-1} + \left( -r_d - 2\frac{k_{11}}{h_1^2} - \frac{k_{22}}{h_2^2} \right) W_{i, j} + \left( \frac{k_2}{2h_2} + \frac{k_{22}}{h_2^2} \right) W_{i, j+1} \right] \\ & + \left[ -\frac{k_{12}}{4h_1h_2} W_{i+1, j-1} + \left( \frac{k_1}{2h_1} + \frac{k_{11}}{h_1^2} \right) W_{i+1, j} + \frac{k_{12}}{4h_1h_2} W_{i+1, j+1} \right] \\ & + O(h_1^2 + h_2^2 + h_1h_2) \end{aligned}$$

- This system of equations can be represented in a matrix form as

$$\begin{aligned} -A_1 \Phi_1 + C_1 \Phi_2 &= F_1 \\ -A_j \Phi_{j-1} + C_j \Phi_j - B_j \Phi_{j+1} &= F_j, \quad j = 2, N_2 - 1 \\ -A_N \Phi_{N_2-1} + C_N \Phi_N &= F_N \end{aligned}$$

and can be effectively solved by a block LU factorization.

# Validation of the scheme against the Heston model

## Heston model

$$\begin{aligned}dS &= S\mu dt + S\sqrt{\nu}dW^{(1)} & (69) \\d\nu &= \kappa(\Theta - \nu)dt + \sigma_V\sqrt{\nu}dW^{(2)},\end{aligned}$$

where  $W^{(1)}$  and  $W^{(2)}$  are Brownian motions with correlation  $\rho$ ,  $\kappa$  is the rate of mean-reversion,  $\sigma$  is the volatility of variance  $\nu$ ,  $\theta$  is a long term run value,  $\mu$  is the drift. All parameters in the Heston model assume to be constant.

## ■ Heston model

$$\begin{aligned}dS &= S\mu dt + S\sqrt{\nu}dW^{(1)} \\d\nu &= \kappa(\Theta - \nu)dt + \sigma_V\sqrt{\nu}dW^{(2)},\end{aligned}\tag{69}$$

where  $W^{(1)}$  and  $W^{(2)}$  are Brownian motions with correlation  $\rho$ ,  $\kappa$  is the rate of mean-reversion,  $\sigma$  is the volatility of variance  $\nu$ ,  $\theta$  is a long term run value,  $\mu$  is the drift. All parameters in the Heston model assume to be constant.

- As can be seen this equation looks exactly like our 2d PIDE if one omits the integral term, put  $\sigma_V = 1$ ,  $\Theta = 1$  and use values of  $r_d$  and  $r_f$  that are twice these values in the Heston model.



## ■ Heston model

$$\begin{aligned}dS &= S\mu dt + S\sqrt{\nu}dW^{(1)} \\d\nu &= \kappa(\Theta - \nu)dt + \sigma_V\sqrt{\nu}dW^{(2)},\end{aligned}\tag{70}$$

where  $W^{(1)}$  and  $W^{(2)}$  are Brownian motions with correlation  $\rho$ ,  $\kappa$  is the rate of mean-reversion,  $\sigma$  is the volatility of variance  $\nu$ ,  $\theta$  is a long term run value,  $\mu$  is the drift. All parameters in the Heston model assume to be constant.

■ As can be seen this equation looks exactly like our 2d PIDE if one omits the integral term, put  $\sigma_V = 1$ ,  $\Theta = 1$  and use values of  $r_d$  and  $r_f$  that are twice these values in the Heston model.

■ Benchmarks: At  $\rho = 0$  and  $r_d = r_f$  an analytical solution and calculator are available at

<http://www.wilmott.com/messageview.cfm?catid=10&threadid=9893&STARTPAGE=1>.

## ■ Heston model

$$\begin{aligned}dS &= S\mu dt + S\sqrt{\nu}dW^{(1)} \\d\nu &= \kappa(\Theta - \nu)dt + \sigma_V\sqrt{\nu}dW^{(2)},\end{aligned}\tag{71}$$

where  $W^{(1)}$  and  $W^{(2)}$  are Brownian motions with correlation  $\rho$ ,  $\kappa$  is the rate of mean-reversion,  $\sigma$  is the volatility of variance  $\nu$ ,  $\theta$  is a long term run value,  $\mu$  is the drift. All parameters in the Heston model assume to be constant.

■ As can be seen this equation looks exactly like our 2d PIDE if one omits the integral term, put  $\sigma_V = 1$ ,  $\Theta = 1$  and use values of  $r_d$  and  $r_f$  that are twice these values in the Heston model.

■ Benchmarks: At  $\rho = 0$  and  $r_d = r_f$  an analytical solution and calculator are available at

<http://www.wilmott.com/messageview.cfm?catid=10&threadid=9893&STARTPAGE=1>.

■ General case - FD solution of T.Kluge 2002

<http://kluge.in-chemnitz.de/tools/pricer/>

# Validation - analytical results

In our tests we used parameters of the Heston model given in the below Table. We also used  $h_1 = h_2 = 0.01$ ,  $\theta = 0.01$  and  $V_{max} = 0.5$ .

$T$	$r_d = r_f$	$K$	$L$	$H$	$\sigma_V$	$\kappa$	$\Theta$	$\rho$
0.3	0.05	100	90	110	0.2	5	0.02	0

# Validation - analytical results

In our tests we used parameters of the Heston model given in the below Table. We also used  $h_1 = h_2 = 0.01$ ,  $\theta = 0.01$  and  $V_{max} = 0.5$ .

$T$	$r_d = r_f$	$K$	$L$	$H$	$\sigma_V$	$\kappa$	$\Theta$	$\rho$
0.3	0.05	100	90	110	0.2	5	0.02	0

Surprisingly, it turned out that condensing mesh points in the vicinity of the barriers make the agreement worse. However, the accuracy significantly improves if we condense mesh points around the strike, the initial level of the volatility, and in the vicinity of the boundary  $v_i = 0$ . So in further calculations we used  $\alpha_L = \alpha_H = 0.1$ ,  $\alpha_K = \alpha_0 = \alpha_{v0} = 20$ .

# Validation - analytical results

In our tests we used parameters of the Heston model given in the below Table. We also used  $h_1 = h_2 = 0.01, \theta = 0.01$  and  $V_{max} = 0.5$ .

$T$	$r_d = r_f$	$K$	$L$	$H$	$\sigma_V$	$\kappa$	$\Theta$	$\rho$
0.3	0.05	100	90	110	0.2	5	0.02	0

Surprisingly, it turned out that condensing mesh points in the vicinity of the barriers make the agreement worse. However, the accuracy significantly improves if we condense mesh points around the strike, the initial level of the volatility, and in the vicinity of the boundary  $v_i = 0$ . So in further calculations we used  $\alpha_L = \alpha_H = 0.1, \alpha_K = \alpha_0 = \alpha_{v0} = 20$ .

$S$	92	94	96	98	100	102	104	106	108
A	0.20174	0.39878	0.58045	0.72785	0.81660	0.82353	0.73487	0.55263	0.29645
BDF2	0.20079	0.39716	0.57897	0.72468	0.81511	0.82385	0.73625	0.55458	0.29768
CN	0.20060	0.39683	0.57861	0.72445	0.81514	0.82417	0.73678	0.55513	0.29803
A-BDF2	0.00095	0.00162	0.00148	0.00317	0.00149	-0.00032	-0.00138	-0.00195	-0.00123
A-CN	0.00114	0.00195	0.00184	0.00340	0.00146	-0.00064	-0.00191	-0.00250	-0.00158

Table 1: Comparison of the analytical and our BDF2 and CN numerical solutions at  $V_0 = 0.03$

# Validation - analytical results

$V_0$	0.0001	0.001	0.01	0.02	0.03	0.04	0.05	0.06	0.1	0.4
A	1.36083	1.34814	1.18203	0.98650	0.81660	0.67575	0.55992	0.46453	0.22154	0.00088
BDF2	1.36642	1.36203	1.18424	0.98596	0.81512	0.67399	0.55813	0.46278	0.22067	0.00088
CN	1.36499	1.36057	1.18352	0.98575	0.81514	0.67412	0.55831	0.46300	0.22095	0.00090
A-BDF2	-0.00559	-0.01389	-0.00221	0.00054	0.00148	0.00176	0.00179	0.00175	0.00087	0
A-CN	-0.00416	-0.01243	-0.00149	0.00075	0.00146	0.00163	0.00161	0.00153	0.00059	-0.00002

Table 2: Comparison of the analytical and our BDF2 and CN numerical solutions at  $S = 100$

# Validation - analytical results

$V_0$	0.0001	0.001	0.01	0.02	0.03	0.04	0.05	0.06	0.1	0.4
A	1.36083	1.34814	1.18203	0.98650	0.81660	0.67575	0.55992	0.46453	0.22154	0.00088
BDF2	1.36642	1.36203	1.18424	0.98596	0.81512	0.67399	0.55813	0.46278	0.22067	0.00088
CN	1.36499	1.36057	1.18352	0.98575	0.81514	0.67412	0.55831	0.46300	0.22095	0.00090
A-BDF2	-0.00559	-0.01389	-0.00221	0.00054	0.00148	0.00176	0.00179	0.00175	0.00087	0
A-CN	-0.00416	-0.01243	-0.00149	0.00075	0.00146	0.00163	0.00161	0.00153	0.00059	-0.00002

Table 2: Comparison of the analytical and our BDF2 and CN numerical solutions at  $S = 100$

In the below tests we used  $r_d = 0.05$ ,  $r_f = 0.03$ ,  $\rho = -0.5$ ,  $V_0 = 0.03$ .

$S$	92	94	96	98	100	102	104	106	108
Kluge	0.27799	0.54906	0.78915	0.95899	1.02546	0.97333	0.81068	0.56790	0.28458
BDF2	0.27846	0.54913	0.78888	0.95785	1.02812	0.97914	0.81804	0.57451	0.28795
Abs. error	-0.00047	-0.00007	0.00027	0.00114	-0.00266	-0.00581	-0.00736	-0.00661	-0.00337

# Validation - analytical results

$V_0$	0.0001	0.001	0.01	0.02	0.03	0.04	0.05	0.06	0.1	0.4
A	1.36083	1.34814	1.18203	0.98650	0.81660	0.67575	0.55992	0.46453	0.22154	0.00088
BDF2	1.36642	1.36203	1.18424	0.98596	0.81512	0.67399	0.55813	0.46278	0.22067	0.00088
CN	1.36499	1.36057	1.18352	0.98575	0.81514	0.67412	0.55831	0.46300	0.22095	0.00090
A-BDF2	-0.00559	-0.01389	-0.00221	0.00054	0.00148	0.00176	0.00179	0.00175	0.00087	0
A-CN	-0.00416	-0.01243	-0.00149	0.00075	0.00146	0.00163	0.00161	0.00153	0.00059	-0.00002

Table 2: Comparison of the analytical and our BDF2 and CN numerical solutions at  $S = 100$

In the below tests we used  $r_d = 0.05, r_f = 0.03, \rho = -0.5, V_0 = 0.03$ .

$S$	92	94	96	98	100	102	104	106	108
Kluge	0.27799	0.54906	0.78915	0.95899	1.02546	0.97333	0.81068	0.56790	0.28458
BDF2	0.27846	0.54913	0.78888	0.95785	1.02812	0.97914	0.81804	0.57451	0.28795
Abs. error	-0.00047	-0.00007	0.00027	0.00114	-0.00266	-0.00581	-0.00736	-0.00661	-0.00337

Same at  $S = 100$ .

$V_0$	0.0001	0.001	0.01	0.02	0.03	0.04	0.05	0.06	0.1	0.4
Kluge	0.69085	1.38448	1.55071	1.26475	1.02546	0.83472	0.68288	0.56085	0.26418	-0.01741
BDF2	1.78635	1.83843	1.56712	1.27043	1.02812	0.83532	0.68158	0.55801	0.25625	0.00092
Abs. error	-1.09550	-0.45395	-0.01641	-0.00568	-0.00266	-0.00060	0.00130	0.00284	0.00793	-0.01833



# Validation - analytical results

$V_0$	0.0001	0.001	0.01	0.02	0.03	0.04	0.05	0.06	0.1	0.4
A	1.36083	1.34814	1.18203	0.98650	0.81660	0.67575	0.55992	0.46453	0.22154	0.00088
BDF2	1.36642	1.36203	1.18424	0.98596	0.81512	0.67399	0.55813	0.46278	0.22067	0.00088
CN	1.36499	1.36057	1.18352	0.98575	0.81514	0.67412	0.55831	0.46300	0.22095	0.00090
A-BDF2	-0.00559	-0.01389	-0.00221	0.00054	0.00148	0.00176	0.00179	0.00175	0.00087	0
A-CN	-0.00416	-0.01243	-0.00149	0.00075	0.00146	0.00163	0.00161	0.00153	0.00059	-0.00002

Table 2: Comparison of the analytical and our BDF2 and CN numerical solutions at  $S = 100$

In the below tests we used  $r_d = 0.05, r_f = 0.03, \rho = -0.5, V_0 = 0.03$ .

$S$	92	94	96	98	100	102	104	106	108
Kluge	0.27799	0.54906	0.78915	0.95899	1.02546	0.97333	0.81068	0.56790	0.28458
BDF2	0.27846	0.54913	0.78888	0.95785	1.02812	0.97914	0.81804	0.57451	0.28795
Abs. error	-0.00047	-0.00007	0.00027	0.00114	-0.00266	-0.00581	-0.00736	-0.00661	-0.00337

Same at  $S = 100$ .

$V_0$	0.0001	0.001	0.01	0.02	0.03	0.04	0.05	0.06	0.1	0.4
Kluge	0.69085	1.38448	1.55071	1.26475	1.02546	0.83472	0.68288	0.56085	0.26418	-0.01741
BDF2	1.78635	1.83843	1.56712	1.27043	1.02812	0.83532	0.68158	0.55801	0.25625	0.00092
Abs. error	-1.09550	-0.45395	-0.01641	-0.00568	-0.00266	-0.00060	0.00130	0.00284	0.00793	-0.01833

1. Negative option price at  $V_0 = 0.4$ . 2. Different boundary conditions at the

origin  $V = 0$ .

# Results

## Numerical results

---

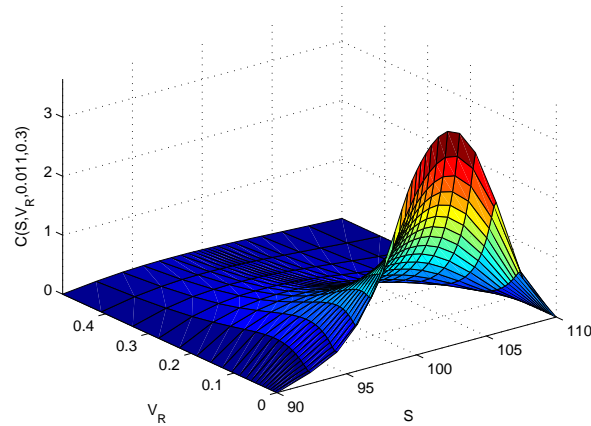
- Splitting for two-step FD schemes - how to choose  $C^{n-1}(x, V_R, V_L, \theta)$ ?  
Our numerical experiments showed that the total solution is very sensitive to this choice. Therefore, we use a one-step method - the Crank-Nicholson method. But still 2nd order in time and space.

- Splitting for two-step FD schemes - how to choose  $C^{n-1}(x, V_R, V_L, \theta)$ ?  
Our numerical experiments showed that the total solution is very sensitive to this choice. Therefore, we use a one-step method - the Crank-Nicholson method. But still 2nd order in time and space.
- Also despite theoretically the order of operators  $L_1$  and  $L_2$  doesn't matter, our test showed that there exist a slight difference in the results when the order of the operators is changed. That is why we used the sequence  $L_1, L_2$  at every odd step in time, and the sequence  $L_2, L_1$  at every even step in time, thus providing an additional symmetry of splitting.

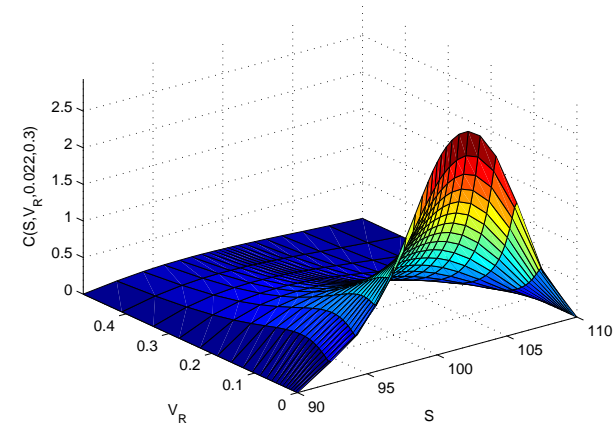
- Splitting for two-step FD schemes - how to choose  $C^{n-1}(x, V_R, V_L, \theta)$ ?  
Our numerical experiments showed that the total solution is very sensitive to this choice. Therefore, we use a one-step method - the Crank-Nicholson method. But still 2nd order in time and space.
- Also despite theoretically the order of operators  $L_1$  and  $L_2$  doesn't matter, our test showed that there exist a slight difference in the results when the order of the operators is changed. That is why we used the sequence  $L_1, L_2$  at every odd step in time, and the sequence  $L_2, L_1$  at every even step in time, thus providing an additional symmetry of splitting.
- Further first we consider a pure diffusion process with no jumps. This is a barrier call option which parameters were given in the Table before, and  $r_d = 0.05, r_f = 0.02, \sigma = 0.2, \rho_R = 0.7, \rho_L = -0.2, \kappa = 0.1$ . We choose the computational domain as  $\mathcal{L} \leq x \leq \mathcal{H}, 0 \leq V_R < 0.5 = V_{max}, 0 \leq V_L < 0.5 = V_{max}$ . Parameters of the grid are same as in the previous section. The grid steps in space and time are  $h_1 = 0.05, h_2 = 0.025, \theta = 0.02$ .

# Results - no jumps

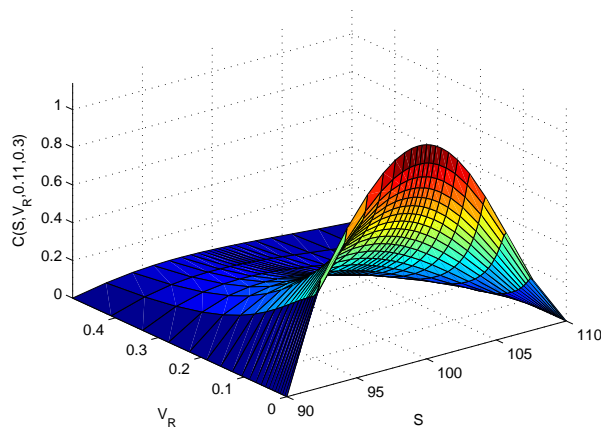
The double barrier option value as a function of  $S$  and  $V_R$ . Parameters are:  $\sigma = 0.2, \rho_R = 0.7, \rho_L = -0.2, \kappa = 0.1$ . Other parameters - see Table.



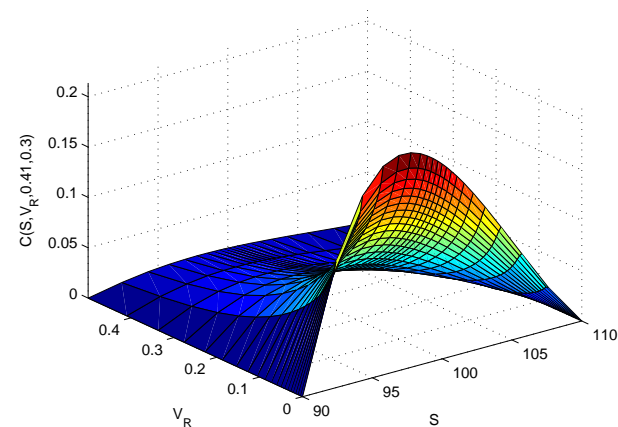
○  $V_L = 0.011$



○  $V_L = 0.022$



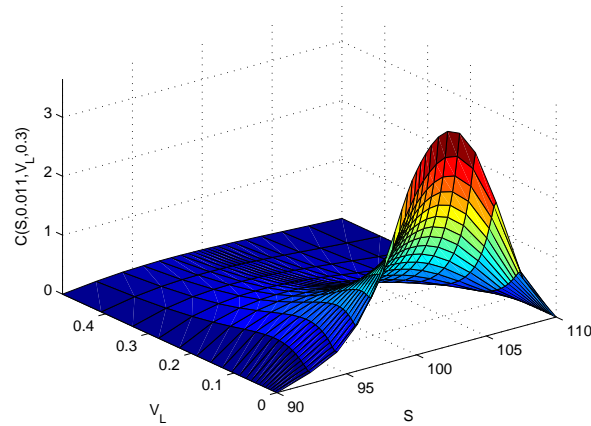
○  $V_L = 0.11$



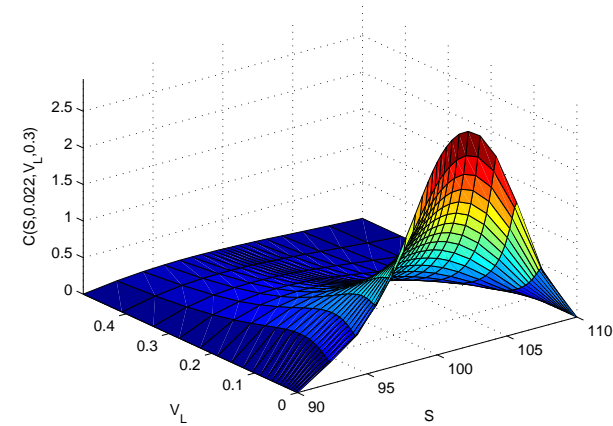
○  $V_L = 0.41$

# Results - no jumps

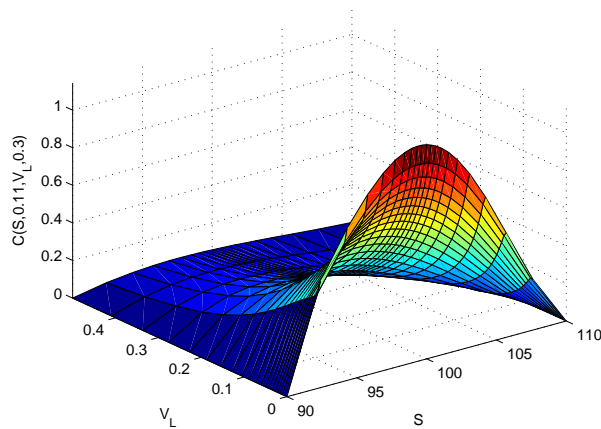
The double barrier option value as a function of  $S$  and  $V_L$ . Parameters are:  $\sigma = 0.2, \rho_R = 0.7, \rho_L = -0.2, \kappa = 0.1$ . Other parameters - see Table.



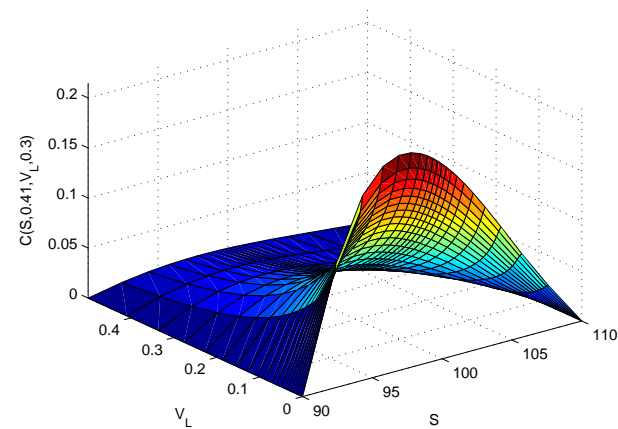
()  $V_R = 0.011$



()  $V_R = 0.022$



()  $V_R = 0.11$

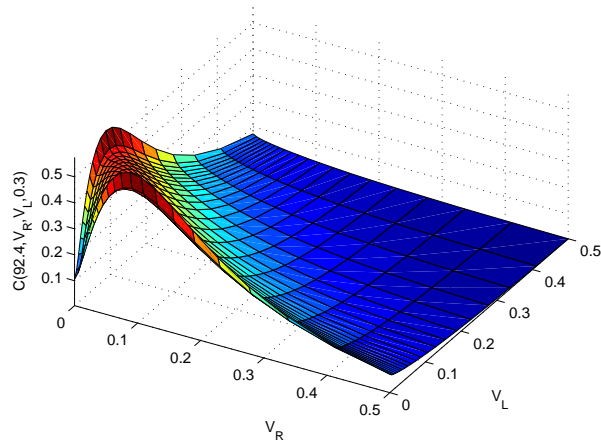


()  $V_R = 0.41$

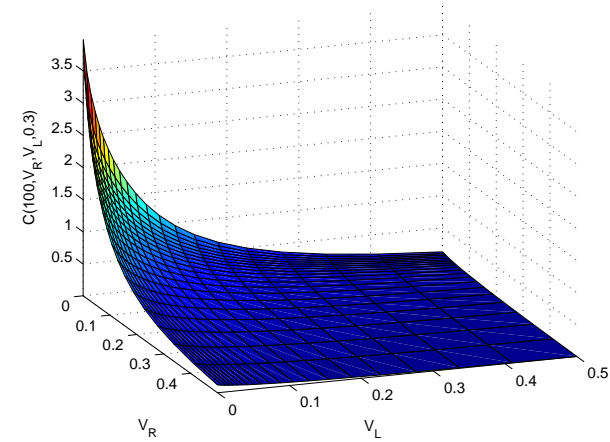
# Results - no jumps

The double barrier option value as a function of  $V_R$  and  $V_L$ .

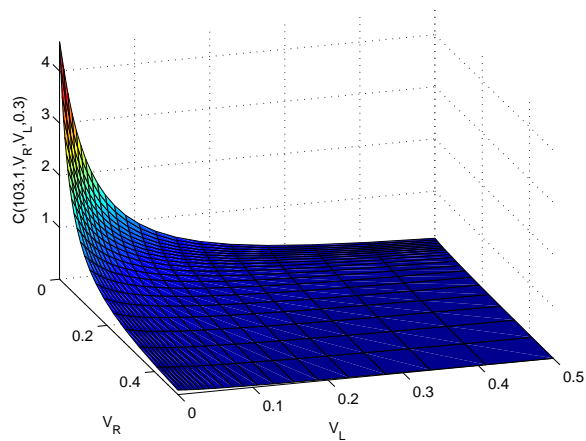
Parameters of the test are:  $\sigma = 0.2, \rho_R = 0.7, \rho_L = -0.2, \kappa = 0.1$ .



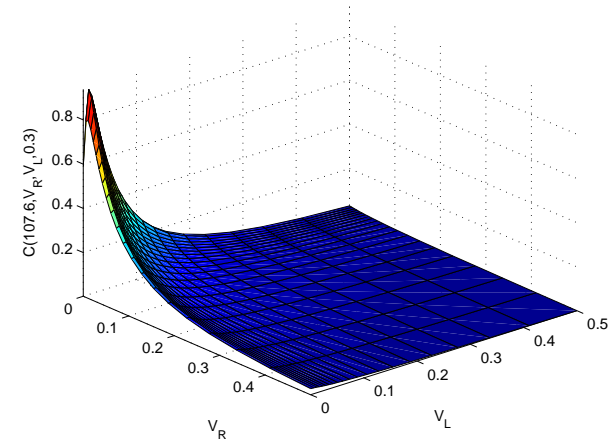
()  $S = 92.4$



()  $S = 100 - \text{ATM}$



()  $S = 103.1$



()  $S = 107.6$



## Results - the Kou model

---

- Next we consider a jump diffusion process where jumps of the finite activity. To simulate these jumps we use a Kou double exponential model with the following values of parameters:  $\alpha = -1$ ,  $\nu_j = 2$ ,  $\lambda = 10$ .

## Results - the Kou model

- Next we consider a jump diffusion process where jumps of the finite activity. To simulate these jumps we use a Kou double exponential model with the following values of parameters:  $\alpha = -1, \nu_j = 2, \lambda = 10$ .
- Again we price a barrier call option which parameters were given in the Table, and  $r_d = 0.05, r_f = 0.02, \sigma = 0.2, \rho_R = 0.7, \rho_L = -0.2$ . We choose the computational domain as  $\mathcal{L} \leq x \leq \mathcal{H}, 0 \leq V_R < 0.5 = V_{max}, 0 \leq V_L < 0.4 = V_{max}$ . Parameters of the grid are same as in the previous section. The grid steps in space and time are  $h_1 = 0.05, h_2 = 0.025, \theta = 0.02$ .

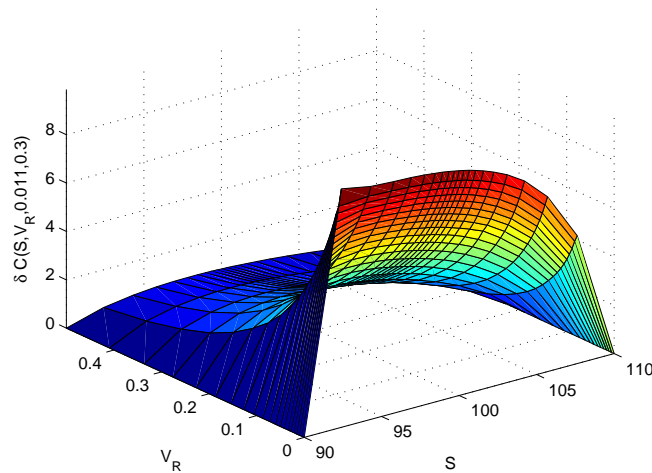
- Next we consider a jump diffusion process where jumps of the finite activity. To simulate these jumps we use a Kou double exponential model with the following values of parameters:  $\alpha = -1, \nu_j = 2, \lambda = 10$ .
- Again we price a barrier call option which parameters were given in the Table, and  $r_d = 0.05, r_f = 0.02, \sigma = 0.2, \rho_R = 0.7, \rho_L = -0.2$ . We choose the computational domain as  $\mathcal{L} \leq x \leq \mathcal{H}, 0 \leq V_R < 0.5 = V_{max}, 0 \leq V_L < 0.4 = V_{max}$ . Parameters of the grid are same as in the previous section. The grid steps in space and time are  $h_1 = 0.05, h_2 = 0.025, \theta = 0.02$ .
- The results are presented as a difference between the jump-diffusion process and analogous process with no jumps. For convenience we introduce the notation

$$\delta C(S, V_R, V_L, T) = C_j(S, V_R, V_L, T) - C_n(S, V_R, V_L, T)$$

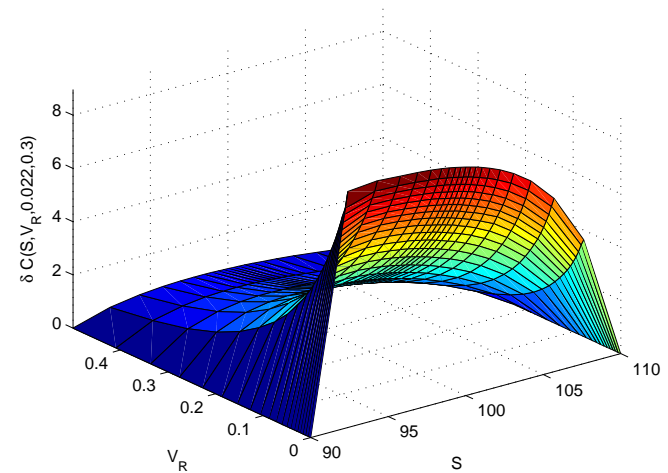
where  $C_j(S, V_R, V_L, T)$  is the option price for the jump-diffusion process and  $C_n(S, V_R, V_L, T)$  is the option price for a pure diffusion process with no jumps.

# Results - the Kou model

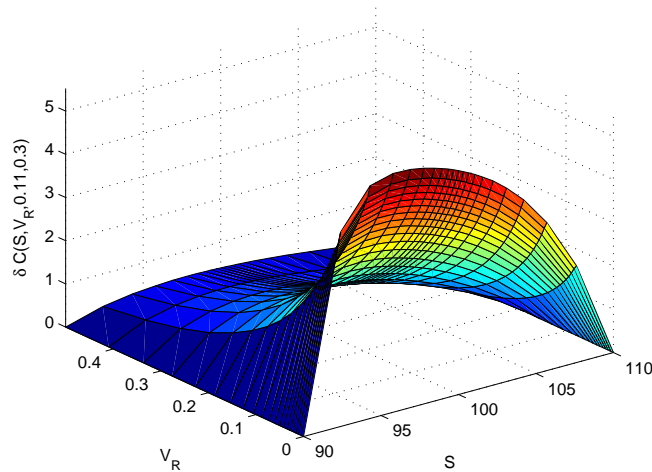
The value of  $\delta C(S, V_R, V_L, T)$  as a function of  $S$  and  $V_R$ . Parameters of the test are:  $\sigma = 0.2, \rho_R = 0.7, \rho_L = -0.2, \kappa = 0.1$



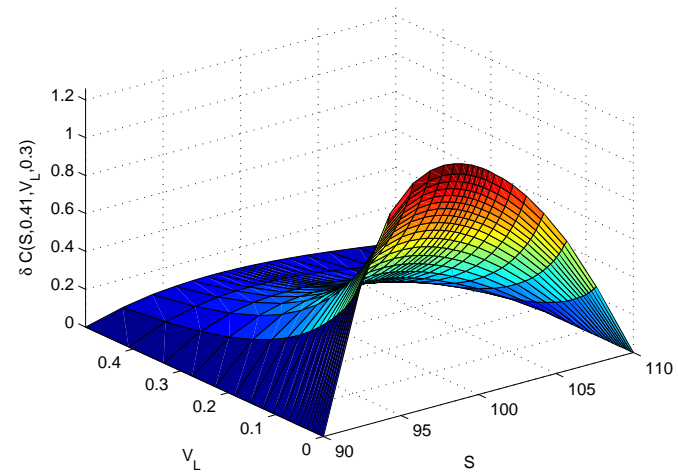
()  $V_L = 0.011$



()  $V_L = 0.022$



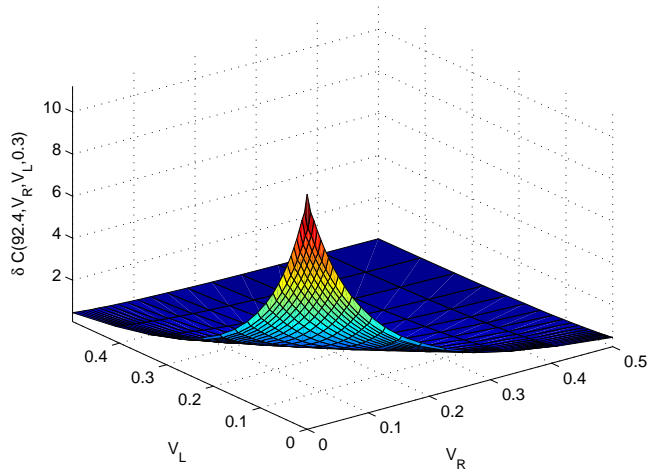
()  $V_L = 0.11$



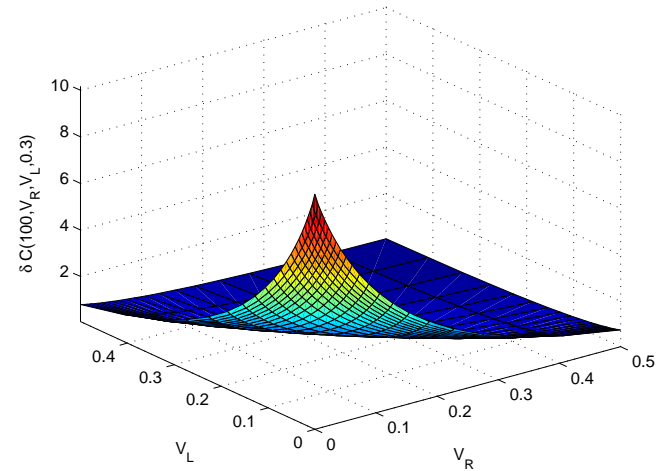
()  $V_L = 0.41$

# Results - the Kou model

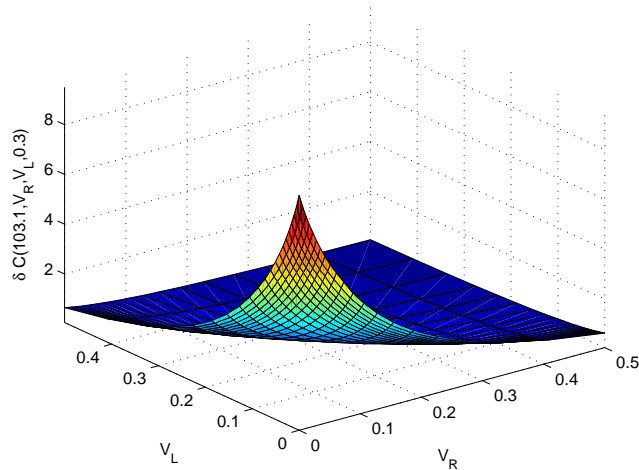
The value of  $\delta C(S, V_R, V_L, T)$  as a function of  $V_R$  and  $V_L$ . Parameters of the test are:  $\sigma = 0.2, \rho_R = 0.7, \rho_L = -0.2, \kappa = 0.1$



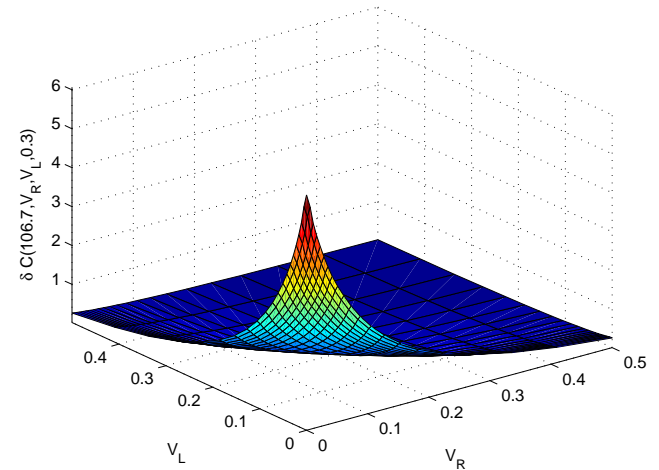
()  $S = 92.4$



()  $S = 100$  - almost ATM



()  $S = 103.1$



()  $S = 107.6$

# Conclusions

# Conclusions

---

- For FX market Carr and Wu proposed a class of models (SSM) that capture both stochastic volatility and skewness. They considered only the European vanilla options while exotics could be of a great interest as well.

# Conclusions

---

- For FX market Carr and Wu proposed a class of models (SSM) that capture both stochastic volatility and skewness. They considered only the European vanilla options while exotics could be of a great interest as well.
- Standard numerical methods are too expensive to price this kind of options - 3d unsteady PIDE.



# Conclusions

---

- For FX market Carr and Wu proposed a class of models (SSM) that capture both stochastic volatility and skewness. They considered only the European vanilla options while exotics could be of a great interest as well.
- Standard numerical methods are too expensive to price this kind of options - 3d unsteady PIDE.
- We attacked this problem by first splitting the original 3d PIDE into two 2d PIDE. This splitting is exact, i.e. doesn't bring any numerical error into the solution.

# Conclusions

---

- For FX market Carr and Wu proposed a class of models (SSM) that capture both stochastic volatility and skewness. They considered only the European vanilla options while exotics could be of a great interest as well.
- Standard numerical methods are too expensive to price this kind of options - 3d unsteady PIDE.
- We attacked this problem by first splitting the original 3d PIDE into two 2d PIDE. This splitting is exact, i.e. doesn't bring any numerical error into the solution.
- We developed a FD scheme for solving 2d PIDE which is of the second order in time and space.

# Conclusions

- For FX market Carr and Wu proposed a class of models (SSM) that capture both stochastic volatility and skewness. They considered only the European vanilla options while exotics could be of a great interest as well.
- Standard numerical methods are too expensive to price this kind of options - 3d unsteady PIDE.
- We attacked this problem by first splitting the original 3d PIDE into two 2d PIDE. This splitting is exact, i.e. doesn't bring any numerical error into the solution.
- We developed a FD scheme for solving 2d PIDE which is of the second order in time and space.
- We used coordinate transformations in order to better resolve the solution at critical points.

- For FX market Carr and Wu proposed a class of models (SSM) that capture both stochastic volatility and skewness. They considered only the European vanilla options while exotics could be of a great interest as well.
- Standard numerical methods are too expensive to price this kind of options - 3d unsteady PIDE.
- We attacked this problem by first splitting the original 3d PIDE into two 2d PIDE. This splitting is exact, i.e. doesn't bring any numerical error into the solution.
- We developed a FD scheme for solving 2d PIDE which is of the second order in time and space.
- We used coordinate transformations in order to better resolve the solution at critical points.
- Validation of the method against the Heston model (analytical and existing numerical solutions) demonstrated its high accuracy.

- For FX market Carr and Wu proposed a class of models (SSM) that capture both stochastic volatility and skewness. They considered only the European vanilla options while exotics could be of a great interest as well.
- Standard numerical methods are too expensive to price this kind of options - 3d unsteady PIDE.
- We attacked this problem by first splitting the original 3d PIDE into two 2d PIDE. This splitting is exact, i.e. doesn't bring any numerical error into the solution.
- We developed a FD scheme for solving 2d PIDE which is of the second order in time and space.
- We used coordinate transformations in order to better resolve the solution at critical points.
- Validation of the method against the Heston model (analytical and existing numerical solutions) demonstrated its high accuracy.
- As it was expected computation of the integral term takes majority of time and essentially slows down the calculations. For instance, at our PC computation of one step in time of the pure diffusion process takes about a second while same computation for the jump-diffusion process takes about 70 seconds.

Thank you!